PIONEER-CLIMAX TREE COMPETITION MODELS

By

Shuichi Sakai

B. Sc. University of British Columbia, 1995

A THESIS SUBMITTED IN PARTIAL FULFILLMENT OF

THE REQUIREMENTS FOR THE DEGREE OF

MASTER OF SCIENCE

in

THE FACULTY OF GRADUATE STUDIES

DEPARTMENT OF MATHEMATICS

INSTITUTE OF APPLIED MATHEMATICS

We accept this thesis as conforming

to the required standard

THE UNIVERSITY OF BRITISH COLUMBIA

June 1997

In presenting this thesis in partial fulfilment of the requirements for an advanced degree at the University of British Columbia, I agree that the Library shall make it freely available for reference and study. I further agree that permission for extensive copying of this thesis for scholarly purposes may be granted by the head of my department or by his or her representatives. It is understood that copying or publication of this thesis for financial gain shall not be allowed without my written permission.

Department of Mathematics

The University of British Columbia
Vancouver, Canada

Date June 17 1997

DE-6 (2/88)

Abstract

Tree species can be broadly categorized into two kinds: pioneer and climax. Pioneer species are ones that survive under low population densities, but progressively do worse as densities increase. Climax species, on the other hand, need some degree of neighboring population to survive, and have a maximum fitness at a unique population density, whereafter fitness decreases with increased competition. This thesis examines models of competition between these two species both in continuous and discrete time. Whereas popular belief is that the pioneer species become extinct with competition, the models studied here suggest the possibility of coexistence, either in a stable equilibrium or a periodic solution. Simple genetical variations on one or both species are also considered for their effects on coexistence. It is found that genetic variety can be a crucial factor in achieving coexistence between the two species.

Table of Contents

List of Figures

Acknowledgement

I wish to thank my supervisor, Professor Wayne Nagata for his patience, Professors Gene Namkoong and James F. Selgrade for their advice, and Dr. Lynn Van Coller for the instructions on the software packages.

Chapter 1

Introduction

1.1 Overview and motivation

Mathematical and numerical analysis can produce interesting and useful qualitative insights into many biological models, as has been shown in many papers in the past, including those by May [9],[10]. Dynamical systems theory in particular is very well suited for population dynamics. In this thesis I examine some simple models of competition between two tree species in both continuous and discrete time. As well, continuous-time and discrete-time competition models that involve simple genetic variation in one or both species are studied using analytical techniques and a software package.

Pioneer species are the types of trees that first appear, for example, after a forest fire: they are hardy and thrive in low population densities. Certain varieties of pine and poplar are considered pioneer. Soon after the growth of pioneer trees, a successionary species enters the scene and enjoys the presence of pioneer trees because of the suitable environment that they provide, such as better soil condition and protection from weather. However, a pioneer species suffers from an increase in population density, and its fitness is reduced. The successionary species are also called climax species, because they have some optimal population density for their growth. Oak and maple are examples of the climax type. After the total population has grown to certain size, however, newcomers also start to suffer from competition for nutrients and space.

Typically, the pioneers species are believed to be excluded with competition. However,

under certain circumstances coexistence is possible . There have been some papers [3],[4], that examined conditions for exclusion or coexistence and possible manipulation that may lead to stable coexistence, using simple dynamical system models. This thesis surveys these results, then adds another factor of simple genetic variation in one or both species to see what effects the variation may have on the competition. Specifically, we explore cases where stable coexistence is possible when all genotypes are present whereas neither homozygotes alone can produce stable coexistence.

While all the models represented here are very simplistic, ignoring any stochastic or spatial effects, it is hoped that qualitative behavior is persistent under such perturbations. This hope is mathematically reasonable, because it is known in dynamical systems theory that many qualitative phenomena, such as Hopf bifurcation, are robust under perturbations: the terms ignored in simple models would be 'perturbations' to the model, which, if sufficiently small, should not affect the overall behavior. Comparison with field research is very difficult because experimental estimations of density dependent replacement rates are difficult to obtain, and cannot be precise. Furthermore, destabilizing spatial effects and large stochastic events (forest fires and clear-cutting, for example) would affect any behavior that is governed by the dynamical equations. While it would be very complicated to model the stochastic and spatial effects, one can argue at least from these studies that pioneer exclusion is not always a valid assumption, and that the simplest genetic variations can affect the qualitative behavior of the system.

1.2 Generic models

One of the earliest mathematical biology models by Malthus (see, for example, Murray [11]) states that a population would continue to grow at a rate proportional to its size. That is, given a population whose size is characterized by a density variable X, it grows

as

$$\frac{dX}{dt} = \mu X \tag{1.1}$$

for a continuous-time model (ODE), and

$$X \longmapsto \mu X \tag{1.2}$$

for a discrete-time model (map). The proportionality parameter μ is often called the *matlthusian parameter* and incorporates death rate and birth rate. The parameter is considered constant for the simplest model, indicating unlimited resources for growth. The solution is exponential growth for either continuous or discrete time models. For more realistic models, this parameter is not constant: as the population grows, the natural resources becomes scarce, the death rate rises, and the growth rate naturally diminishes. Thus the next step is to consider a malthusian parameter that is a function of population density. That is, $\mu = \mu(X)$, and any realistic function must satisfy $\lim_{X\to\infty} \mu(X) < 0$ for an ODE, and $0 \leq \lim_{X\to\infty} \mu(X) < 1$ for maps. These functions are also called *fitness functions*, since they measure the fitness of a population.

There are good reasons for studying both the continuous-time and discrete-time models as it is done in this thesis. The continuous-time systems, in general, are easier to analyze than the discrete-time models, and it is in principle better to approach a model by steps from the simpler to the more complex. Continuous-time models, however, may not be sufficiently accurate for discretely reproducing biological populations such as trees, which reproduce once a year. A system of ODEs may be more suitable for other organisms that reproduce in relatively short time-intervals (bacteria, for example).

The equations (1.1) and (1.2) are for dynamics involving a single homogeneous population. For dynamics that involves interaction between two or more populations, the fitness of each population must be functions of the size of each population. So if $X_i, i = 1, \ldots, n$ are the densities of n interacting populations, the populations have

fitnesses $\mu_i(X_1, X_2, ..., X_n)$. Instead of considering fitnesses as functions of n variables, they can be thought of as functions of what are known as *total weighted densities*, Z_i which are defined as:

$$Z_i = c_{i1}X_1 + c_{i2}X_2 + ... + c_{in}X_n = \sum_{j=1}^{n} c_{ij}X_j. \tag{1.3}$$

The coefficients c_{ij} measure the density effect of the jth population on the ith population, and these simplify notation and analyses considerably. The equations of dynamics are now written as:

$$\frac{dX_i}{dt} = g_i(Z_i)X_i \tag{1.4}$$

for the continuous-time system, and

$$X_i \longmapsto f_i(Z_i)X_i \tag{1.5}$$

for the discrete-time map (also called diffeomorphism). This weighted density variable is employed by most recent papers on the subject concerned in this thesis [4], [13], [14], [18],[20], [21], [22].

1.3 Population genetics

The later chapters consider simple genetic variations on one or both tree species. The dynamics involving genetic variation are characterized by additional variables called *genetic frequencies*, which are the number of gametes or individuals carrying an allele divided by the total numbers of gametes. The genetic variation that we consider has two alleles at one locus for a sexually reproducing diploid. Alleles are genes that appear in pairs and which determine the phenotype of the individual. Suppose A and a are the two alleles. Then there are three possible combinations: AA, Aa and aa. The AA and aa genotypes are called *homozygotes* while the Aa combination is called a *heterozygote*. Each of these

genotypes may possess different characteristics, and their fitnesses can be varied: at a certain population density one genotype might be more fit, while at another density, a different genotype may be superior. Sometimes the heterozygote, possessing both alleles, exhibits a fitness between those of the two homozygotes, in which case it is said that we have *partial dominance* in the heterozygote. When the heterozygote of the population is more fit than both homozygotes, we have what is called *overdominance* or *heterozygote superiority.* Thirdly, when the heterozygote is less fit than both homozygotes, we have *underdominance* or *heterozygote inferiority.* Heterozygote superiority, for example, was thought to have been a necessary condition for existence of periodic solutions in a single population. For the case of two alleles with random mating, it can be shown that species maintain what is known as the Hardy-Weinberg Ratio, a fixed ratio between the three types. It is also true that with random mating, a population that begins with a genotype-ratio that deviates from the Hardy-Weinberg goes to the ratio in one generation. Knowledge of the ratio allows distribution of the genotypes to be characterized by a single variable, p, the genetics frequency of the A allele. This means that $p = 1$ is a population dominated completely by the AA genotype, while a population with genetic frequency $p = 0$ has only the aa genotype. These two extreme cases are called *fixations.* While a population has not fixated, that is, $0 < p < 1$, then the population is said to be *polymorphic.*

Now consider a one-species genetic variation model, such as one of those studied in Van Coller [23]. Each of the three genotypes has a distinct fitness function denoted by μ_{AA}, μ_{Aa} and μ_{aa}. Then the variables X, the total population density and p, the genetic frequency propagates in time for the continuous-time case as follows:

$$\frac{dp}{dt} = p(\mu - \mu_A), \tag{1.6}$$

$$\frac{dX}{dt} = \mu X, \tag{1.7}$$

where μ_a and μ_A are defined as

$$\mu_A = p\mu_{AA} + (1-p)\mu_{Aa}, \tag{1.8}$$

$$\mu_a = p\mu_{Aa} + (1-p)\mu_{aa}, \tag{1.9}$$

and μ is the average population fitness defined as

$$\mu = p\mu_A + (1-p)\mu_a. \tag{1.10}$$

For the discrete-time model, equations (1.8),(1.9) and (1.10) are the same, and the variables X and p propagate in time as

$$p \longmapsto p\frac{\mu_A}{\mu}, \tag{1.11}$$

$$X \longmapsto \mu X. \tag{1.12}$$

The details of these derivations are found in Crow and Kimura [1]. For the genetic population models, the fitnesses μ_{ij} can be functions of the population density as well as the gene frequency, however, all fitness functions considered in this thesis depend on population density only.

1.4 Thesis outline

The first half of this thesis gives an overview of other published papers on the subject. Chapter 2 looks at the basic models of pioneer-climax competition in continuous time. Results of previous analyses are summarized, then a particular example is examined using a phase-plotting and bifurcation analysis software package called XPPAUT. Chapter 3 involves similar models, but in discrete time. Again, some theoretical analyses is reviewed before continuing with an example model and its numerical analysis. Chapter 4 begins to explore a simple genetic variation in the pioneer species in continuous time. The

theoretical analysis that has been done on a generic two-species competition with a simple genetic variation is covered for the pioneer-climax case, then XPPAUT again is used to examine a particular simple model. An analysis analogous to that used in chapter 4 is used for the discrete-time model in chapter 5. Finally, a brief analysis and a numerical example for the four-dimensional case, where genetic variation is added to both competing species, is presented in chapter 6. Since most of the analysis is done using the numerical package XPPAUT, the background and the mechanics of this package is described briefly in appendix A. Some examples of computer listings for various models are also placed in the appendix.

Chapter 2

Simple continuous-time competition

Very simple models of continuous-time pioneer-climax competition are studied in papers of Sumner [21], [22], Selgrade and Namkoong [18]. The papers concentrate mainly on the analysis of a Hopf bifurcation and the resulting periodic orbit and its stability. It had been believed that in an undisturbed pioneer-climax competitive system, the climax species would always exclude the pioneer species. There are, however, actual forests where pioneer species persist (see [18] for further references). The papers mentioned above show that contrary to the belief, stable coexistence or even stable fluctuation of population densities via Hopf bifurcation is possible. Using very simple models, they derive conditions for the occurrence of Hopf bifurcations and compute Floquet exponents of the bifurcating periodic solution to determine the stability of the solution. All the papers mentioned above use the weighted total density as variables for the fitness functions. Sumner's paper [22] goes beyond the basic model to add harvesting or planting terms to explore what is required to attain stable coexistence or a limit cycle where none was possible without the control terms. The basic results are reiterated here, but the control aspect of the model is not covered.

In the first section, the basic models are introduced, and summary of the theoretical analysis is presented. The next section then gives a numerical example of a particular model using XPPAUT.

2.1 Model equations

Denote by M the population density of the pioneer species and by N that of the climax species. Then the system of ODEs for the two variables are

$$\frac{dM}{dt} = M\mu(Z), \tag{2.1}$$

$$\frac{dN}{dt} = N\eta(W), \tag{2.2}$$

where Z and W are the weighted total densities defined by

$$\begin{pmatrix} Z \\ W \end{pmatrix} = C \begin{pmatrix} M \\ N \end{pmatrix}, \tag{2.3}$$

with

$$C = \begin{pmatrix} c_{11} & c_{12} \\ c_{21} & c_{22} \end{pmatrix}. \tag{2.4}$$

The matrix C is called the interaction matrix, as mentioned in the introduction, and it measures the degree of intraspecific and interspecific competition for the two species (for example c_{11} is the intraspecific competition for the pioneer species and c_{12} is the interspecific competition for the pioneer). For the fitness function $\mu(Z)$ to correspond to a pioneer species, we take it to be a monotonically decreasing function with $\mu(0) > 0$, μ equal to 0 at exactly one place, say at $Z_1 > 0$, and thus $\mu(Z) < 0$ for $Z > Z_1$. As a consequence of these conditions, $\mu'(Z_1)$ must be negative. For N to be a climax species we require its fitness function, η be unimodal (one-hump). Further, we assume $\eta(0) < 0$, that η has one peak at W^* where $\eta(W^*) > 0$, and that $\eta(W)$ is equal 0 at exactly two places, at W_1 and W_2, with $0 < W_1 < W_2$. As consequence, we have $\eta'(W_1) > 0$ and $\eta'(W_2) < 0$. See figure 2.1 for typical examples of pioneer and climax fitness functions. An interior equilibrium occurs when the two isoclines $\mu(Z) = \mu(M, N) = 0$ and $\eta(W) = \eta(M, N) = 0$ intersect. These can be found by solving the system of linear

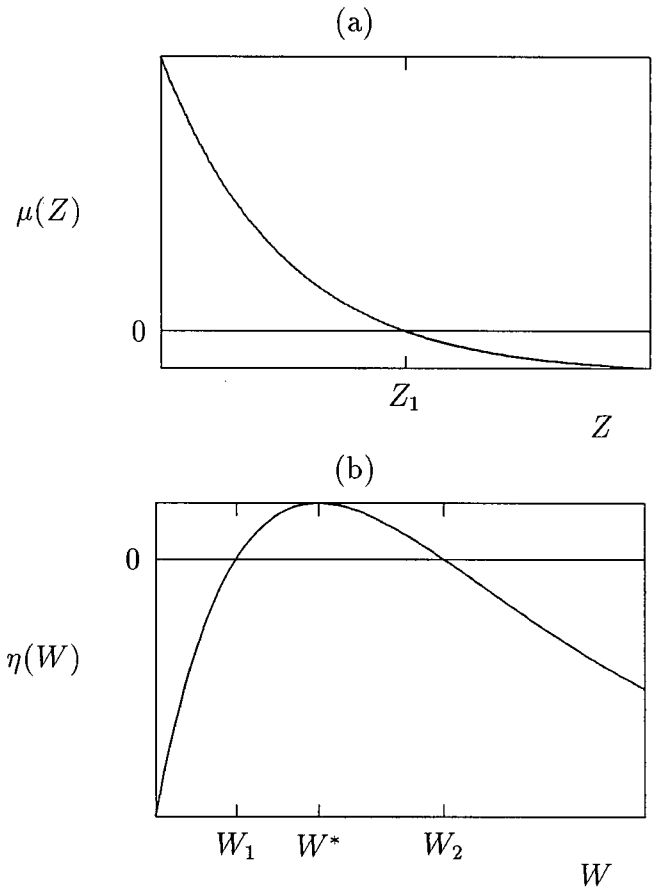

Figure 2.1: Typical (a) pioneer and (b) climax fitness functions for ODE models

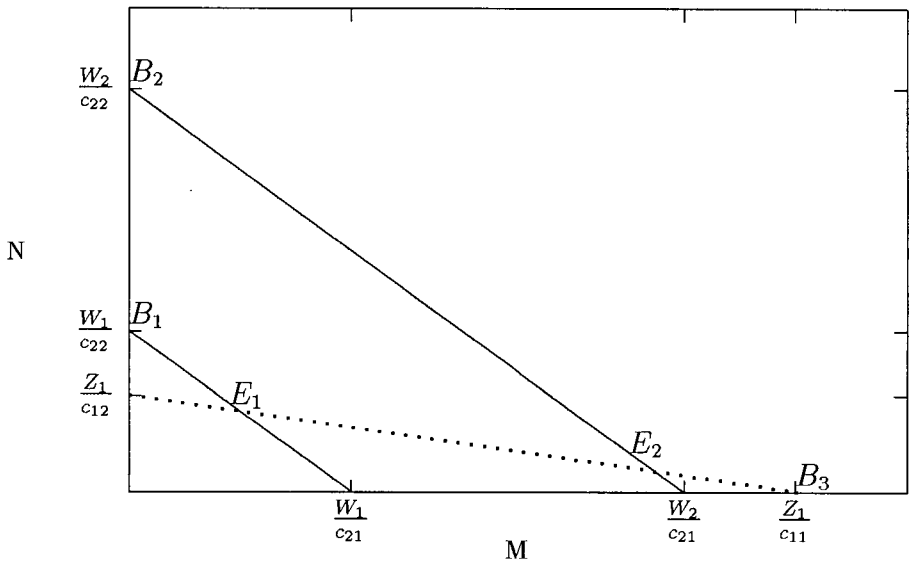

Figure 2.2: Equations $W = W_{1,2}$ and $Z = Z_1$

equations $\{Z = c_{11}M + c_{12}N = Z_1, W = c_{21}M + c_{21}N = W_{1,2}\}$. This is illustrated in figure 2.2. From the figure one can see that there are two different interior equilibria, E_1 corresponding to a smaller equilibrium W_1 for the climax species, and E_2 corresponding to W_2. The equilibria are

$$\begin{aligned} M_i &= \frac{c_{22}Z_1 - c_{12}W_i}{\det C}, \\ N_i &= \frac{c_{11}W_i - c_{21}Z_1}{\det C}. \end{aligned} \tag{2.5}$$

There are also boundary equilibria $B_{1,2} = \{M = 0, N = W_{1,2}/c_{22}\}$ and $B_3 = \{M = Z_1/c_{11}, N = 0\}$ that correspond to the exclusion of either species.

To look at the local stability of these equilibria, the Jacobian of the vector field is found:

$$J(x) = \begin{pmatrix} \mu & 0 \\ 0 & \eta \end{pmatrix} + \begin{pmatrix} M\frac{d\mu}{dZ} & 0 \\ 0 & N\frac{d\eta}{dW} \end{pmatrix} \begin{pmatrix} c_{11} & c_{12} \\ c_{21} & c_{22} \end{pmatrix}, \tag{2.6}$$

where x is the vector $(M, N)^T$. At an equilibrium, $\mu = \eta = 0$, so (2.6) becomes

$$J(E_i) = \begin{pmatrix} c_{11}M\frac{d\mu}{dZ} & c_{12}M\frac{d\mu}{dZ} \\ c_{21}N\frac{d\eta}{dW} & c_{22}N\frac{d\eta}{dW} \end{pmatrix}. \tag{2.7}$$

To determine the eigenvalues at an equilibrium, we consider the trace and the determinant of $J(E_i)$:

$$\sigma = tr\,J(E_i) = M_i c_{11}\mu'(Z_1) + N_i c_{22}\eta'(W_i), \tag{2.8}$$

$$\Delta = \det J(E_i) = M_i N_i \mu'(Z_1)\eta'(W_i)\det C. \tag{2.9}$$

Since the eigenvalues are then

$$\lambda_{1,2} = \frac{1}{2}[\sigma \pm \sqrt{\sigma^2 - 4\Delta}], \tag{2.10}$$

the conditions for stability are $\sigma < 0$ and $\Delta > 0$. Since $\mu'(Z_1) < 0$ and $\eta'(W_1) > 0$, E_1 is stable only if $\det C < 0$, which corresponds to the interspecific competition being greater than the intraspecific competition. Similarly, since $\eta'(W_2) < 0$, E_2 is stable only if $\det C > 0$, corresponding to intraspecific competition being greater than the interspecific competition.

The equilibrium E_2 corresponds to pure competition, where the equilibrium is either stable coexistence or mutual exclusion. Since σ at E_2 is always negative, there is no Hopf bifurcation. On the other hand, E_1 behaves like the interior equilibrium of a predator-prey system. Near this equilibrium, the 'predator' climax species benefits from the increase in population of either species, while the 'prey' pioneer always suffers. If $\det C < 0$, then the sign of σ determines the stability of E_1, and Hopf bifurcation may occur at parameter values where $\sigma = 0$.

2.2 Hopf bifurcation analysis at E_1

For a Hopf bifurcation to occur as parameters change, a pair of complex conjugate eigenvalues of the Jacobian at E_1 must cross the imaginary axis. That is to say, the real part of the eigenvalues must change sign. To ensure that the eigenvalues of $J(E_1)$ have nonzero imaginary parts, we must have

$$\sigma^2 < 4\Delta. \tag{2.11}$$

So if $\det C < 0$ and $\sigma = 0$, this condition holds. The first condition is the same as that for the stability of E_1, and second occurs naturally at the bifurcation point. If these conditions are met, then Hopf bifurcation could occur at parameter values that gives $\sigma = trDF(E_1) = 0$. Using (2.8) and (2.5) gives

$$\sigma = \frac{1}{\det C}[(c_{22}Z_1 - c_{12}W_1)c_{11}\mu'(Z_1) + (c_{11}W_1 - c_{21}Z_1)c_{22}\eta'(W_1)]. \tag{2.12}$$

We choose c_{11} and c_{22} as bifurcation parameters, which is reasonable from a biological perspective, since the parameters are self-depressive terms which may possibly be adjusted by the management of such factors as inter-plant spacing (see [18]). Thus if c_{11} is used as the bifurcation parameter, then bifurcation occurs at

$$c_{11} = \frac{c_{21}c_{22}Z_1\eta'(W_1)}{(c_{22}Z_1 - c_{12}W_1)\mu'(Z_1) + c_{22}W_1\eta'(W_1)}, \tag{2.13}$$

and if c_{22} is used, the bifurcation occurs at

$$c_{22} = \frac{c_{11}c_{12}W_1\mu'(Z_1)}{(c_{11}Z_1 - c_{21}W_1)\eta'(W_1) + c_{11}Z_1\mu'(Z_1)}. \tag{2.14}$$

Another condition needed for Hopf bifurcation to occur is one of the following:

$$\frac{d\sigma}{dc_{11}} = \frac{(c_{22}Z_1 - c_{12}W_1)\mu'(Z_1) + c_{22}W_1\eta'(W_1)}{\det C} > 0, \tag{2.15}$$

or

$$\frac{d\sigma}{dc_{22}} = \frac{(c_{11}W_1 - c_{21}Z_1)\eta'(W_1) + c_{11}Z_1\mu'(Z_1)}{\det C} > 0. \tag{2.16}$$

These conditions mean that the eigenvalues cross the imaginary axis with non-zero speed with respect to the varying parameters. It is clear that $\frac{d\sigma}{dc_{11}} < 0$ and $\frac{d\sigma}{dc_{22}} > 0$, because the numerators in (2.5) are negative and $\det C < 0$. Thus Hopf bifurcation occurs, and E_1 becomes unstable as c_{11} is decreased, or if c_{22} is increased.

The periodic orbit resulting from the Hopf bifurcation may or may not be stable. Stability is determined by a parameter β_2 (see Hassard et al. [6] for a formula), which is derived from the third order normal form of the vector field. The parameter is given as

$$\begin{aligned} 8\beta_2 &= \frac{c_{11}^2 W_1 \mu''(Z_1)}{c_{22} N_1} + \frac{c_{22} Z_1 \eta''(W_1)}{M_1} + c_{11} N_1 \det C \eta'(W_1)[\mu''/\mu']'(Z_1) \\ &\quad - c_{22} N_1 \det C \eta'(W_1)[\eta''/\eta']'(W_1) \end{aligned} \tag{2.17}$$

For this calculation, c_{12} and c_{21} have been taken to be 1 by rescaling. If $\beta_2 > 0$ then the orbit is unstable, and if $\beta_2 < 0$ then the orbit is locally asymptotically stable. $\beta_2 = 0$ corresponds to critical Hopf bifurcation. Selgrade and Namkoong [18] in their paper use this parameter to show the existence of a Hopf bifurcation and a resulting stable periodic cycle for an exponential model similar to the one presented in the following section.

2.3 Numerical example using XPPAUT

Here we consider exponential fitness functions of the form

$$\mu(Z) = e^{(a-Z)} - 1 \tag{2.18}$$

$$\eta(W) = We^{(b-W)} - 1. \tag{2.19}$$

Assuming that $c_{21} = c_{12} = 1$ after appropriate scaling, we are left with four parameters c_{11}, c_{22}, a and b. Using c_{11} as the bifurcation parameter, figure 2.3 shows the transition from a stable equilibrium to a stable periodic orbit to an unstable equilibrium as c_{11} decreases. The bifurcation involving the break-up of the periodic orbit is a global one,

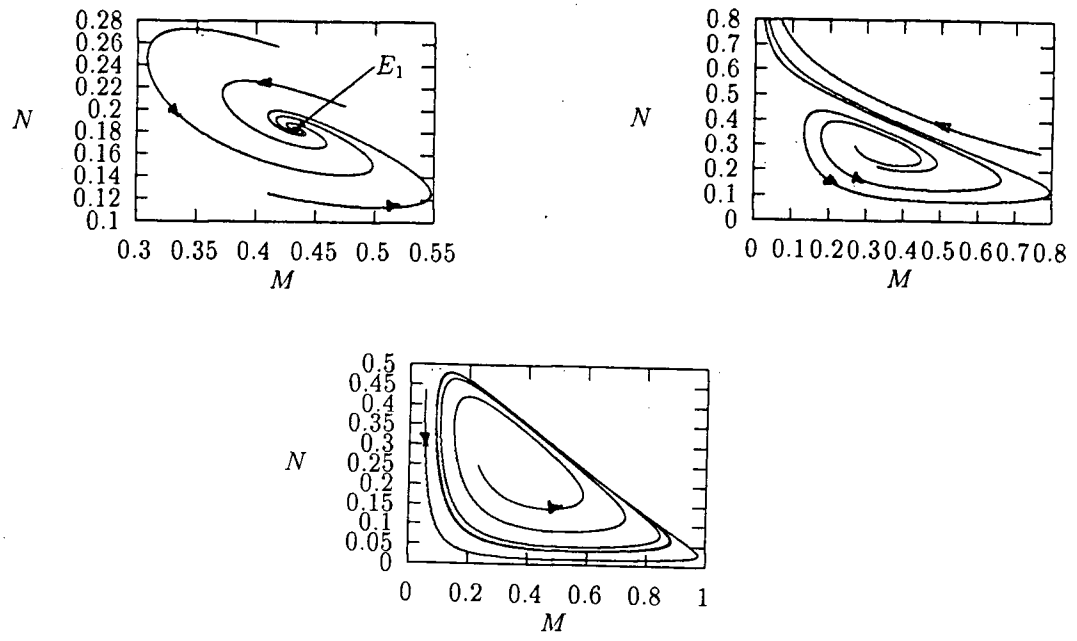

Figure 2.3: Hopf bifurcation at E_1 for $a = 0.4$, $b = 1.1$, $c_{22} = 1$. The phase portrait on the left shows a stable equilibrium at $c_{11} = 0.45$. Hopf bifurcation occurs at $c_{11} = 0.4141$. The middle phase portrait shows a stable periodic orbit for $c_{11} = 0.38$. $c_{11} = 0.35$ in the right phase portrait, when orbit has vanished.

probably a saddle-loop bifurcation (see Kuznetsov [7]), and this cannot be detected using local analysis. Figure 2.4 shows the bifurcation diagram in c_{11} from XPPAUT. As c_{11} is decreased through a bifurcation value, E_1 becomes unstable and stable periodic orbit (solid dots) appear. The amplitude of oscillation, characterized by the maximum and minimum of M on the diagram, increases until the orbit vanishes in the global bifurcation. Note that when c_{11} is further decreased E_2 appears, however, it is unstable since $\det C < 0$ still. The interior equilibria E_1 and E_2 cease to exist in the positive quadrant at the branching points on B_3. Finally, a two-parameter continuation of the Hopf bifurcation at E_1 is demonstrated in figure 2.5 in which c_{22} is chosen as the second parameter. The arrow on the figure indicates the direction of Hopf bifurcation as either c_{11} is decreased, or c_{22} is increased.

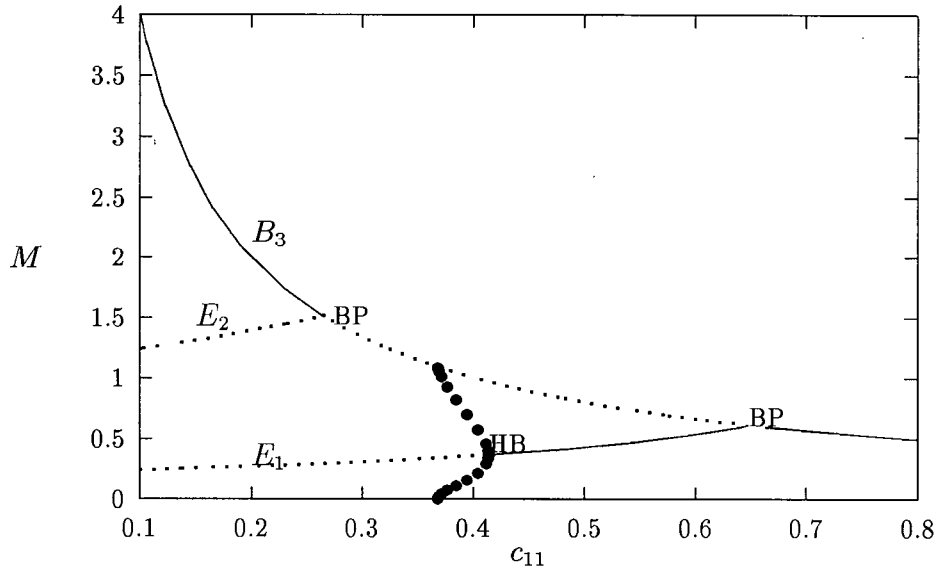

Figure 2.4: Bifurcation diagram in c_{11} for $a = 0.4$, $b = 1.1$, and $c_{22} = 1$. Thick lines indicate stability while the dotted lines are unstable. Hopf bifurcation is marked HB, and branching points are marked BP

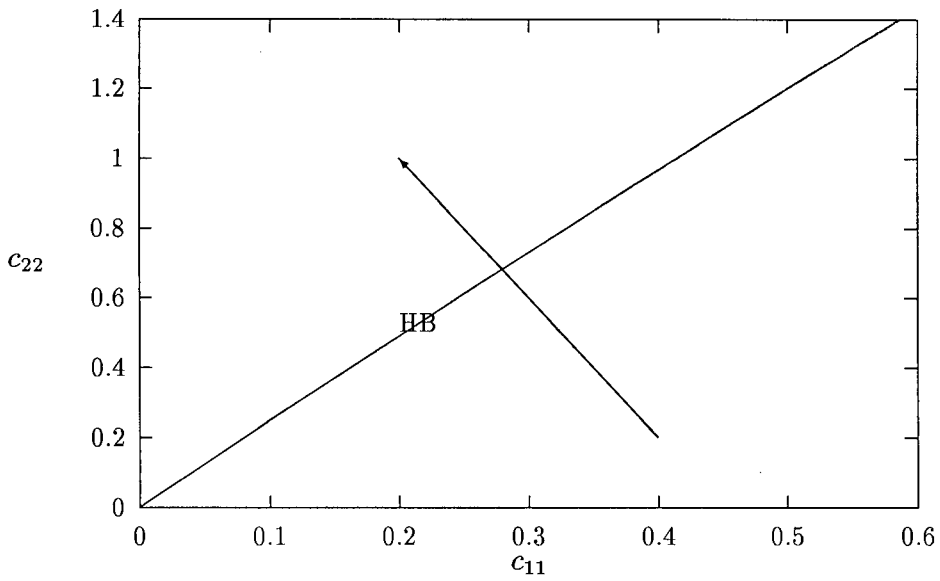

Figure 2.5: Two-parameter bifurcation in c_{11} and c_{22}. The other parameters kept constant as before.

2.4 Summary

The papers referenced in this chapter were able to show that for many parameter combinations, a simple model of pioneer-climax competition exhibits stable coexistence, contrary to popular belief. The numerical example in the last section verified these results. However, none of the papers referenced achieves correspondence with real forests by giving any biologically 'reasonable' parameter values, which would give us the likelihood of the events occurring, or the environments which would produce the events.

Chapter 3

Simple discrete-time competition

In this chapter, the simple model is extended to discrete-time maps. Models specific to pioneer-climax discrete-time competition are found in papers by Franke and Yakubu [3],[4], and Selgrade [19],[20]. The goals of these papers are same as the ones mentioned at the beginning of previous chapter, i.e., to find conditions for stable coexistence or for the existence of an invariant circle between the pioneer and climax species. However, the continuous time-models are replaced by discrete-time models. This change makes theoretical analysis a little more difficult, but the results are basically the same. Conditions for stable interior equilibria, Hopf bifurcations for maps (also called Neimark-Sacker bifurcations) and the stability of the resulting invariant circles are explored. Also, again, factors of harvesting and planting control terms are added in [14] and [24], but these are not covered in this thesis. The next section describes the main results of theoretical analysis, and the section after that gives a Hopf bifurcation analysis at an equilibrium, then an actual numerical example using XPPAUT in the final section.

3.1 Model equation

The continuous-time system of chapter 1 now becomes a local diffeomorphism:

$$(M, N) \longmapsto (M\mu(Z), N\eta(W)) \tag{3.1}$$

where, again, μ and η are smooth functions of the weighted total densities Z and W. Interior equilibria are found by solving the equations $\{\mu(Z) = 1, \eta(W) = 1\}$. Again

there are at most two interior equilibria corresponding to the solutions of $\{Z = Z_1, W = W_i\}, i = 1, 2$, where $\mu(Z_1) = 1$ and $\eta(W_{1,2}) = 1$. The solutions are exactly the same as before:

$$\begin{aligned} M_i &= \frac{c_{22}Z_1 - c_{12}W_i}{\det C}, \\ N_i &= \frac{c_{11}W_i - c_{21}Z_1}{\det C}. \end{aligned} \tag{3.2}$$

The Jacobian, also, is as before:

$$J(x) = \begin{pmatrix} \mu & 0 \\ 0 & \eta \end{pmatrix} + \begin{pmatrix} M\frac{d\mu}{dZ} & 0 \\ 0 & N\frac{d\eta}{dW} \end{pmatrix} \begin{pmatrix} c_{11} & c_{12} \\ c_{21} & c_{22} \end{pmatrix}, \tag{3.3}$$

except now, the first matrix becomes the identity matrix at an equilibrium:

$$J(E_i) = I + \begin{pmatrix} c_{11}M\frac{d\mu}{dZ} & c_{12}M\frac{d\mu}{dZ} \\ c_{21}N\frac{d\eta}{dW} & c_{22}N\frac{d\eta}{dW} \end{pmatrix}. \tag{3.4}$$

The trace σ and determinant Δ of $J(E_i)$ are

$$\sigma = 2 + M_i\mu'(Z_1)c_{11} + N_i\eta'(W_i)c_{22}, \tag{3.5}$$

$$\Delta = 1 + M_i\mu'(Z_1)c_{11} + N_i\eta'(W_i)c_{22} + M_iN_i\mu'(Z_1)\eta'(W_i)\det C. \tag{3.6}$$

The eigenvalues are thus:

$$\begin{aligned} \lambda_{1,2} &= \frac{1}{2}\left[\sigma \pm \sqrt{\sigma^2 - 4\Delta}\right] \\ &= \frac{1}{2}(2 + M_i\mu'(Z_1)c_{11} + N_i\eta'(W_i)c_{22}) \\ &\quad \pm\frac{1}{2}\sqrt{[M_i\mu'(Z_1)c_{11} - N_i\eta'(W_i)c_{22}]^2 - 4M_iN_ic_{12}c_{21}\mu'(Z_1)\eta'(W_1)} \end{aligned} \tag{3.7}$$

For the eigenvalues to have nonzero imaginary parts, it is clear that $\mu'(Z_1)\eta'(W_i) < 0$ is necessary. Since $\mu'(Z_1) < 0$, and $\eta'(W_1) > 0$, only at the smaller interior equilibrium,

E_1 can there be complex eigenvalues. Further, if the eigenvalues are complex conjugates, then the norm squared of the eigenvalues are given by

$$\det \begin{pmatrix} c_{11}M\frac{d\mu}{dZ} & c_{12}M\frac{d\mu}{dZ} \\ c_{21}N\frac{d\eta}{dW} & c_{22}N\frac{d\eta}{dW} \end{pmatrix} = M_1N_1\mu'(Z_1)\eta'(W_1)\det C > 0, \tag{3.8}$$

so $\det C < 0$ is another necessary condition. This condition, again, asserts that interspecific competition is stronger than intraspecific competition.

3.2 Hopf bifurcation for maps

A Hopf bifurcation for discrete-time maps (also known as a Neimark-Sacker bifurcation) occurs when conjugate complex eigenvalues, λ, $\bar{\lambda}$ cross the unit circle at an angle such that $\lambda^n \neq 1$ for $n = 1, 2, 3, 4$. It is known that the complex eigenvalues of the matrix $J(E)$ can lie on the unit circle if and only if $\det J(E) = 1$ and $-2 < trJ(E) < 2$ (see [20] for a proof). These conditions would imply

$$0 > M_1\mu'(Z_1)c_{11} + N_1\eta'(W_1)c_{22}, \quad \text{and} \tag{3.9}$$

$$0 = M_1\mu'(Z_1)c_{11} + N_1\eta'(W_1)c_{22} + M_1N_1\mu'(Z_1)\eta'(W_1)\det C. \tag{3.10}$$

In equation (3.10), the first term is negative and the second and third terms are positive, so the condition may be achieved by either decreasing c_{11} or by increasing c_{22}, however, changes in these parameters also change the values of M_1,N_1 and $\det C$.

If c_{11} is used as the bifurcation parameter, then solving (3.10) and using (3.2), we find that bifurcation occurs at [20]:

$$c_{11} = \frac{c_{22}c_{21}Z_1\eta'(W_1) + c_{21}Z_1(Z_1c_{22} - W_1c_{12})\mu'(Z_1)\eta'(W_1)}{(Z_1c_{22} - W_1c_{12})[1 + W_1\eta'(W_1)]\mu'(Z_1) + c_{22}W_1\eta'(W_1)}. \tag{3.11}$$

Since the numerators in (3.2) are negative at E_2, each term in both the numerator and the denominator of (3.11) is positive. Thus the value given for c_{11} is positive. Similarly,

if c_{22} is used as the bifurcation parameter, bifurcation occurs at:

$$c_{22} = \frac{c_{12}W_1\mu'(Z_1)[c_{11} + \eta'(W_1)(W_1c_{11} - Z_1c_{21})]}{\eta'(W_1)(W_1c_{11} - Z_1c_{21}) + Z_1\mu'(Z_1)[c_{11} + \eta'(W_1)(W_1c_{11} - Z_1c_{21})]}. \tag{3.12}$$

Since from (3.10) and (3.2) we have

$$0 < c_{11} + \eta'(W1)(W_1c_{11} - Z_1c_{21}), \tag{3.13}$$

and hence both numerator and denominator in (3.12) are negative which implies that the value for c_{22} is positive.

To ensure that the eigenvalues cross the unit circle with nonzero speed with respect to changing parameters, we must have $\frac{d|\lambda_\pm|}{c_{11}}$ or $\frac{d|\lambda_\pm|}{c_{22}} \neq 0$. Noting that $|\lambda|^2 = \det J(E_1)$, one can see that

$$\begin{aligned}\frac{d(\det J(E_1))}{dc_{11}} &= \frac{(Z_1c_{22} - W_1c_{12})}{[\det C]^2} \\ &\quad +[c_{21}c_{22}\eta'(W_1) - c_{12}c_{21}\mu'(Z_1) + c_{21}\mu'(Z_1)\eta'(W_1)(Z_1c_{22} - W_2c_{12})]\end{aligned} \tag{3.14}$$

As in the previous chapter, the numerator of the first term is negative, and the denominator is positive, so the derivative is < 0 at bifurcation. Similarly

$$\begin{aligned}\frac{d(\det J(E_1))}{dc_{22}} &= \frac{c_{12}c_{21}\eta'(W_1)(Z_1c_{21} - W_1c_{11})}{[\det C]^2} \\ &\quad + \frac{c_{12}\mu'(Z_1)(W_2c_{11} - Z_1c_{21})[c_{11} + \eta'(W_2)(W_2c_{11} - Z_1c_{21})]}{[\det C]^2}\end{aligned} \tag{3.15}$$

Using (3.2) and (3.13), one can see that the derivative above is positive at bifurcation. Thus Hopf bifurcation occurs as c_{11} is decreased, or as c_{22} is increased. This will be demonstrated in the next section.

An invariant circle typically appears beyond the Hopf bifurcation, and the stability of this invariant circle can be determined by a stability coefficient β which depends on third derivatives of the fitness functions. This coefficient does not reduce to something as simple as that given for the ODE case in chapter 2, so it is omitted here (see Selgrade and Roberds [20] for a detailed derivation).

3.3 Numerical example using XPPAUT

Consider the following exponential fitness functions:

$$\mu(Z) = e^{a-Z}, \tag{3.16}$$

$$\eta(W) = We^{b-W}. \tag{3.17}$$

So again, there are six parameters, c_{ij}, a and b. By appropriate scaling, one can assume that $c_{12} = c_{21} = 1$. Figure 3.1 shows the process of Hopf bifurcation for maps. In the first picture, the interior equilibrium E_2 is stable and attracting. In the second picture, soon after the bifurcation, a stable invariant circle appears. In the third picture, the invariant circle has broken in another global bifurcation. Note that global bifurcation for diffeomorphisms are usually complicated, involving chaos, and thus extremely difficult to analyze by hand (see Kuznetsov[7]). The trajectories on the invariant circle may or may not be periodic: it has been shown (see, for example, [7]) that there are regions in a two-parameter space near the Hopf bifurcation line called *Arnold tongues* where the trajectories on the invariant circle approach periodic orbits as time increases. There are an infinite number of these regions that approach the bifurcation line as narrow tongues. As our generic bifurcation parameter is changed, it goes through an infinite number of Arnold tongues corresponding to different rotation numbers, and thus an infinite number of periodic cycles are born and die as the parameter is varied. The bifurcation diagram in c_{11} is shown in figure 3.2. This is very similar to that found for the continuous-time system, with a Hopf bifurcation point as c_{11} is decreased from a stable equilibrium. The only difference is that XPPAUT cannot draw the minimum and the maximum of the invariant circle after the bifurcation, but this is expected to look similar also, except near global bifurcations. Finally, a similar two-parameter bifurcation diagram for the Hopf bifurcation for maps is shown in figure 3.3. The curved line is the two-parameter Hopf

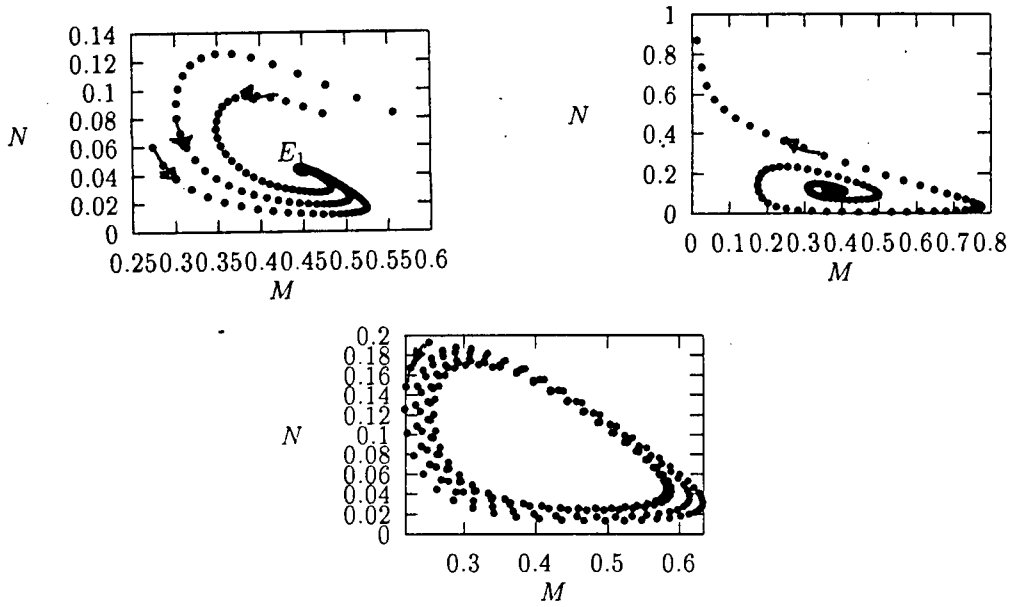

Figure 3.1: Transition from stable equilibrium at E_1 to invariant circle through Hopf bifurcation for maps. The parameters use are $a = 0.3$, $b = 1.1$; $c_{11} = 0.34$ for the first map, $c_{11} = 0.27$ for the second map, and $c_{11} = 0.2$ for the third map.

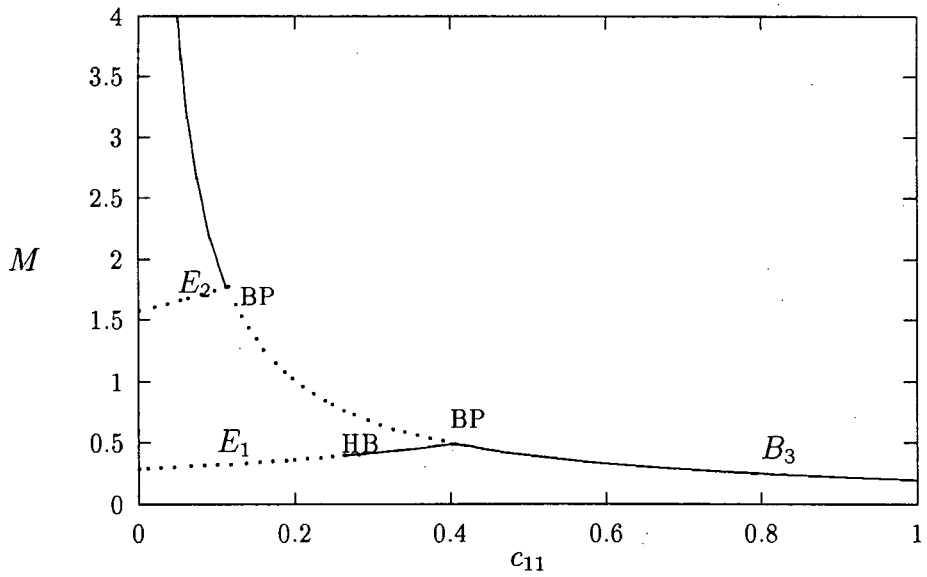

Figure 3.2: Bifurcation diagram for the discrete system in c_{11}. The parameters are $a = 0.3$, $b = 1.1$, $c_{22} = 1$.

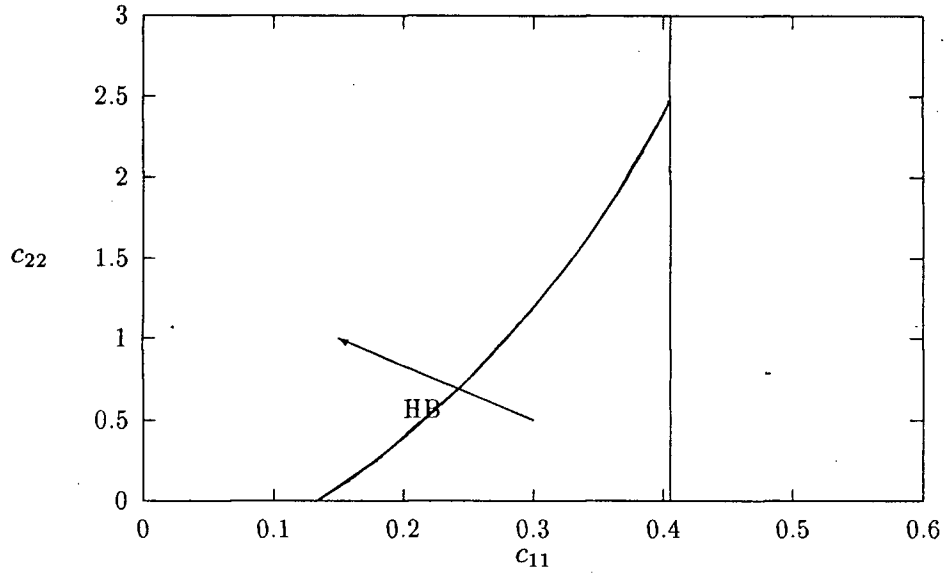

Figure 3.3: Two-parameter bifurcation in c_{11} and c_{22}. To the right of the vertical line, the interior fixed point E_1 does not exist in the positive quadrant. The other parameters are $a = 0.3$ and $b = 1.1$.

bifurcation line, and the vertical line is just the branching point where E_1 ceases to exist in the first quadrant. Arnold tongues are not shown.

3.4 Summary

The discrete-time model is more suited for populations that reproduce in discrete generations. The results obtained in the referenced papers are similar to the ones in the previous chapter: that stable coexistence of the two tree species is possible under many parameter combinations in the form of a stable equilibrium or an invariant circle. The same problem persists, however, that there is no quantitative correspondence with reality. I do not know what the 'reasonable' parameter values may be to test the likelihood of the events described above.

Chapter 4

Continuous-time genetics model

The previous two chapters showed that coexistence of the two species, pioneer and climax, is possible under different conditions, either as a stable equilibrium or as a stable periodic solution. In the next chapters, we examine what the effect of genetic variation might have on existence and stability of equilibria. This is an interesting question, and there have been many papers in the past that examined the question in terms of models of systems of differential and difference equations (for example Roughgarden [12], Levin and Udovic[8], Selgrade and Namkoong [15],[17],[16]). Selgrade and Namkoong [16] for example, investigate cases where either populations are excluded competitively in the absence of genetic variation, but a stable polymorphism exists for competition with genetic variation. They use as examples fitness functions that are linear in the population density variables, and both functions that are independent and dependent of the genetic frequency. They find that for fitness functions that are independent of the genetic frequency, stable polymorphic coexistence is possible for a case where there is global exclusion of the genetic population in its fixation planes. In this chapter, I apply the same questions specific to the pioneer-climax case, adding genetic variation to the pioneer species, and using only fitness functions that are independent of the gene frequency. I have been able to demonstrate using an example, that a stable polymorphic interior equilibrium or cycle are possible, although they vanish on either fixation planes.

Basic models are introduced and a theoretical analysis is done in the next section. In the following section, a special assumption allows the use of an invariant manifold

theorem to show that a stable interior polymorphism and a Hopf bifurcation on the manifold is possible. In the third section a numerical example of this phenomenon is given using XPPAUT.

4.1 Model equations

The following models are extensions of those in chapter 2. With addition of genetic variation in the pioneer species, the dimension of ODE system is increased by one with the introduction of the gene frequency of the A allele, p. As explained in the introduction, the system of equations now becomes

$$\begin{aligned} \frac{dp}{dt} &= p(\mu_A - \mu) = p(1-p)(\mu_A - \mu_a), \\ \frac{dM}{dt} &= \mu M, \\ \frac{dN}{dt} &= \eta N, \end{aligned} \tag{4.1}$$

where μ_a and μ_A are defined as

$$\mu_A = p\mu_{AA} + (1-p)\mu_{Aa}, \tag{4.2}$$

$$\mu_a = p\mu_{Aa} + (1-p)\mu_{aa}, \tag{4.3}$$

and μ is the average population fitness defined as

$$\mu = p\mu_A + (1-p)\mu_a, \tag{4.4}$$

and now there are three distinct fitness functions for each genotype. Only functions of population density are considered in this thesis, although functions involving the genetic frequency p are also possible (see, for example [15]). Thus $\mu_{ij} = \mu_{ij}(M, N)$. Papers such as Selgrade and Namkoong [17] look at a general competition model involving genetic variation, and does most of the analytical ground-work for this chapter. Solutions to

(4.1) are found in the region

$$\mathcal{F} = \{(p, M, N) : 0 \leq p \leq 1, M \geq 0, N \geq 0\}.$$

For an interior equilibrium ($(p, M, N) \in int(\mathcal{F})$) to exist, the heterozygote fitness for the pioneer must be either superior or inferior to both homozygote fitnesses at the equilibrium. That is to say, we have *over-dominance* or *under-dominance* at the equilibrium. At the equilibrium, we have $\mu = \eta = 0$ thus $\mu_A = \mu_a = 0$. The last two conditions imply that the following must be satisfied:

$$p\mu_{AA} + (1-p)\mu_{Aa} = 0, \tag{4.5}$$

$$p\mu_{Aa} + (1-p)\mu_{aa} = 0. \tag{4.6}$$

Solving the above two equations make it necessary that either $\mu_{Aa} > 0 > \mu_{AA}, \mu_{aa}$ or $\mu_{AA}, \mu_{aa} > 0 > \mu_{Aa}$. Since the fitnesses μ_{ij} are independent of p, the following identities can be verified easily:

$$\frac{1}{2}\frac{\partial \mu}{\partial p} = \mu_A - \mu_a, \tag{4.7}$$

$$\frac{1}{2}\frac{\partial^2 \mu}{\partial p^2} = \mu_{AA} - \mu_{aa} - 2\mu_{Aa}. \tag{4.8}$$

Using these, the Jacobian matrix at an internal equilibrium $\mathcal{C}$ is given by

$$J(\mathcal{C}) = \begin{pmatrix} \frac{1}{2}p(1-p)\frac{\partial^2 \mu}{\partial p^2} & p\frac{\partial(\mu_A - \mu)}{\partial M} & p\frac{\partial(\mu_A - \mu)}{\partial N} \\ 0 & M\frac{\partial \mu}{\partial M} & M\frac{\partial \mu}{\partial N} \\ 0 & N\frac{\partial \eta}{\partial M} & N\frac{\partial \eta}{\partial N} \end{pmatrix}. \tag{4.9}$$

The lower right 2×2 matrix of $J(\mathcal{C})$ is called the *ecology matrix* (from [15]) and is denoted by $E(\mathcal{C})$. The eigenvalues of $J(\mathcal{C})$ are $\lambda_1 = \frac{1}{2}p(1-p)\frac{\partial^2 \mu}{\partial p^2} = p(1-p)(\mu_{AA} + \mu_{aa} - 2\mu_{Aa})$, and $\lambda_{2,3}$ are eigenvalues of $E(\mathcal{C})$. For the stability of $\mathcal{C}$, all eigenvalues must have negative real parts. The first eigenvalue λ_1 is purely real, and for $\lambda_1 < 0$, we must clearly have heterozygote superiority: $\mu_{Aa} > 0 > \mu_{AA}, \mu_{aa}$ at the equilibrium.

Following Ginzburg [5], we make a non-degeneracy assumption of the fitness functions:

$$\frac{\partial \mu}{\partial M}\frac{\partial \eta}{\partial N} - \frac{\partial \mu}{\partial N}\frac{\partial \eta}{\partial M} \neq 0, \tag{4.10}$$

which is equivalent to $\det E(\mathcal{C}) \neq 0$ at an isolated equilibrium $\mathcal{C} \in Int\mathcal{F}$. Using the Implicit Function Theorem, one can see that the zero fitness curve locally is the graph of a vector function g of p:

$$\{(p, M, N) : \mu(p, M, N) = \eta(M, N)\} = \{(p, M, N) : (M, N) = g(p)\}. \tag{4.11}$$

The equilibrium $\mathcal{C}$ is a critical point of g since $\partial\mu/\partial p = 0$.

Now consider the eigenvalues of the ecology matrix $E(\mathcal{C})$. The trace and determinant of the matrix are:

$$\sigma = trE(\mathcal{C}) = M\frac{\partial \mu}{\partial M} + N\frac{\partial \eta}{\partial N} \tag{4.12}$$

$$\Delta = \det E(\mathcal{C}) = MN\left(\frac{\partial \mu}{\partial M}\frac{\partial \eta}{\partial N} - \frac{\partial \mu}{\partial N}\frac{\partial \eta}{\partial M}\right) \tag{4.13}$$

For a Hopf bifurcation to occur from the equilibrium $\mathcal{C}$, one must have complex eigenvalues cross the imaginary axis at nonzero speed. For the trace σ to change sign, $\frac{\partial \mu}{\partial M}$ and $\frac{\partial \eta}{\partial N}$ must have opposite signs. Also, since $\frac{\partial \mu}{\partial M}$ and $\frac{\partial \mu}{\partial N}$ are negative (all pioneer genotypes have fitnesses that are monotone decreasing, so any nonnegative sum of the functions must also be monotone decreasing), we must have $\frac{\partial \eta}{\partial M}, \frac{\partial \eta}{\partial N} > 0$. This again indicates a predator-prey interaction. For the pioneer-climax competition, the competition occurs at small densities where the climax species has not yet climaxed.

4.2 Homozygote equality

It is not possible to solve for the interior equilibria in general. However, if we assume a biologically reasonable simplifying condition [17], $\mu_{AA} = \mu_{aa}$ (*homozygote equality*), then

the ODE system can be reduced to two dimensions, and the mean fitness for the pioneer simply becomes the average of the homozygote and heterozygote fitness.

Assuming homozygote equality, it follows that

$$\mu_A - \mu_a = (2p-1)(\mu_{AA} - \mu_{Aa}). \tag{4.14}$$

So if $p = 0.5$ then $\dot{p} = 0$ for all $M, N \geq 0$. A simple coordinate transformation $p = r + \frac{1}{2}$ gives

$$\begin{aligned} \dot{r} &= p(1-p)(2p-1)(\mu_{AA} - \mu_{Aa}) && (4.15)\\ &= (r+\frac{1}{2})(\frac{1}{2}-r)(2r)(\mu_{AA} - \mu_{Aa}) && (4.16)\\ &= r(\mu_{AA} - \mu_{Aa}) + \mathcal{O}(r^2). && (4.17) \end{aligned}$$

Thus, for example, if uniform heterozygote superiority holds throughout $int\mathcal{F}$ (i.e., $\mu_{AA} < \mu_{Aa} - \varepsilon$ throughout $int\mathcal{F}$ for some $\varepsilon > 0$), then the two-dimensional manifold $r = 0$, or equivalently $p = 0.5$, is exponentially stable. Thus the solution to (4.1) reduces to that of

$$\begin{aligned} \dot{M} &= 0.5(\mu_{AA} + \mu_{Aa})M, \\ \dot{N} &= \eta N. \end{aligned} \tag{4.18}$$

Note that the mean fitness in (4.18) is just the average of the genotype fitnesses. The space $\mathcal{P} = \{(p, M, N) : p = 0.5, M > 0, N > 0\}$ is an attracting invariant manifold for each interior equilibrium. Thus a periodic solution which is exponentially stable in $\mathcal{P}$ is also exponentially stable in the full 3-dimensional space, since $\lambda_1 < 0$ is assumed by heterozygote superiority. For this to be true, it is not needed that the plane $\mathcal{P}$ be attracting globally, or in other words, it is not necessary to assume global heterozygote superiority. We only need to assume homozygote equality in a neighborhood of $\mathcal{P}$ and heterozygote superiority at the equilibrium. Moreover, since the bifurcation is persistent

under perturbation, and removing homozygote equality will still leave a Hopf bifurcation. Thus if there exists an example with homozygote equality and with a Hopf bifurcation to a stable periodic solution, there also exist other examples without homozygote equality.

Note that if the interaction coefficients for the genotypes of pioneer are the same, that is if $\mu_{ij} = \mu_{ij}(Z)$, then the reduced system (4.18) can be handled by the analysis of chapter 1 by replacing $\mu(Z) = 0.5[\mu_{AA}(Z) + \mu_{Aa}(Z)]$, since the average of two pioneer fitnesses are also pioneer. All the conditions for the existence of a Hopf bifurcation hold. If the interaction coefficients are different ($\mu_{ij} = \mu_{ij}(Z^{ij})$ and $Z^{ij} = c_{11}^{ij}M + c_{12}^{ij}N$), then the conditions become slightly more complicated. It is no longer possible in general to write the coordinates of the interior equilibria explicitly in terms of Z_1^{ij} and $c_{11}^{ij}, c_{12}^{ij}, c_{21}, c_{22}$, where $\mu_{ij}(Z_1^{ij}) = 0$. The Jacobian at an equilibrium becomes the ecology matrix mentioned above, and no simple condition like $\det C < 0$ can be found. An exception is when the pioneer functions are linear in M and N, and this case is explored in the next section.

4.3 Linear/Quadratic model

Let us assume that a linear fitness function is used for the pioneer species, and a quadratic for the climax fitness. This is especially simple, because under homozygote equality, the average of two linear fitnesses is also a linear fitness. Let

$$\mu_{ij}(Z) = a_{ij} - Z^{ij}, \tag{4.19}$$

$$\eta(W) = b - (W - c)^2, \tag{4.20}$$

then for homozygote equality,

$$\dot{M} = \bar{a} - \bar{Z}, \tag{4.21}$$

$$\dot{N} = b - (W - c)^2, \tag{4.22}$$

where $\bar{a} = (a_{AA} + a_{Aa})/2$, and $\bar{Z} = (Z^{AA} + Z^{Aa})/2$. Also let

$$c_{11} = \frac{1}{2}(c_{11}^{AA} + c_{11}^{Aa}), \tag{4.23}$$

$$c_{21} = \frac{1}{2}(c_{12}^{AA} + c_{12}^{Aa}), \tag{4.24}$$

then $Z = \bar{Z} = c_{11}M + c_{12}N$. So the equilibria (M_i, N_i) are the solutions of

$$Z = c_{11}M + c_{12}N = a, \tag{4.25}$$

$$W = c_{21}M + c_{22}N = \pm\sqrt{b} + c. \tag{4.26}$$

It has already been shown in chapter 2, that only the smaller of the two interior equilibria can undergo a Hopf bifurcation. Thus for E_1

$$M_1 = \frac{c_{22}a - c_{12}(c - \sqrt{b})}{\det C}, \quad N_1 = \frac{c_{11}(c - \sqrt{b}) - c_{21}a}{\det C}. \tag{4.27}$$

Further, noting that $\mu'(Z_1) = -1$ and $\eta'(W_1) = \sqrt{b}$, the bifurcation occurs, using (2.13), at

$$c_{11} = \frac{c_{11}c_{22}\sqrt{b}}{-(c_{22}a - c_{12}(c - \sqrt{b})) + c_{22}(c - \sqrt{b})\sqrt{b}}. \tag{4.28}$$

Figure 4.1 shows trajectories of the linear/quadratic model using XPPAUT, for homozygote equality. Note that p approaches 0.5 monotonically, while on the MN-plane, E_1 is locally asymptotically stable. As one of the bifurcation parameters, c_{11} is decreased (recall that $c_{11} = 1/2(c_{11}^{AA} + c_{11}^{Aa})$, so one can decrease either or both of c_{11}^{AA} and c_{11}^{Aa} to achieve this), the equilibrium goes through a Hopf bifurcation in $\mathcal{P}$, and forms a stable periodic orbit.

This simple example already shows the effect of genetic variation. Although both fixations, $p = 0$ or $p = 1$ are unstable, they are invariant. Thus if, for example, initially $p = 0$ then only the aa genotype is present, and its fitness cannot produce a stable equilibria: the result is exclusion of either species depending on initial values (see figure 4.2 for trajectories on the MN-plane when $p(t = 0) = 1$ or $p(t = 0) = 0$).

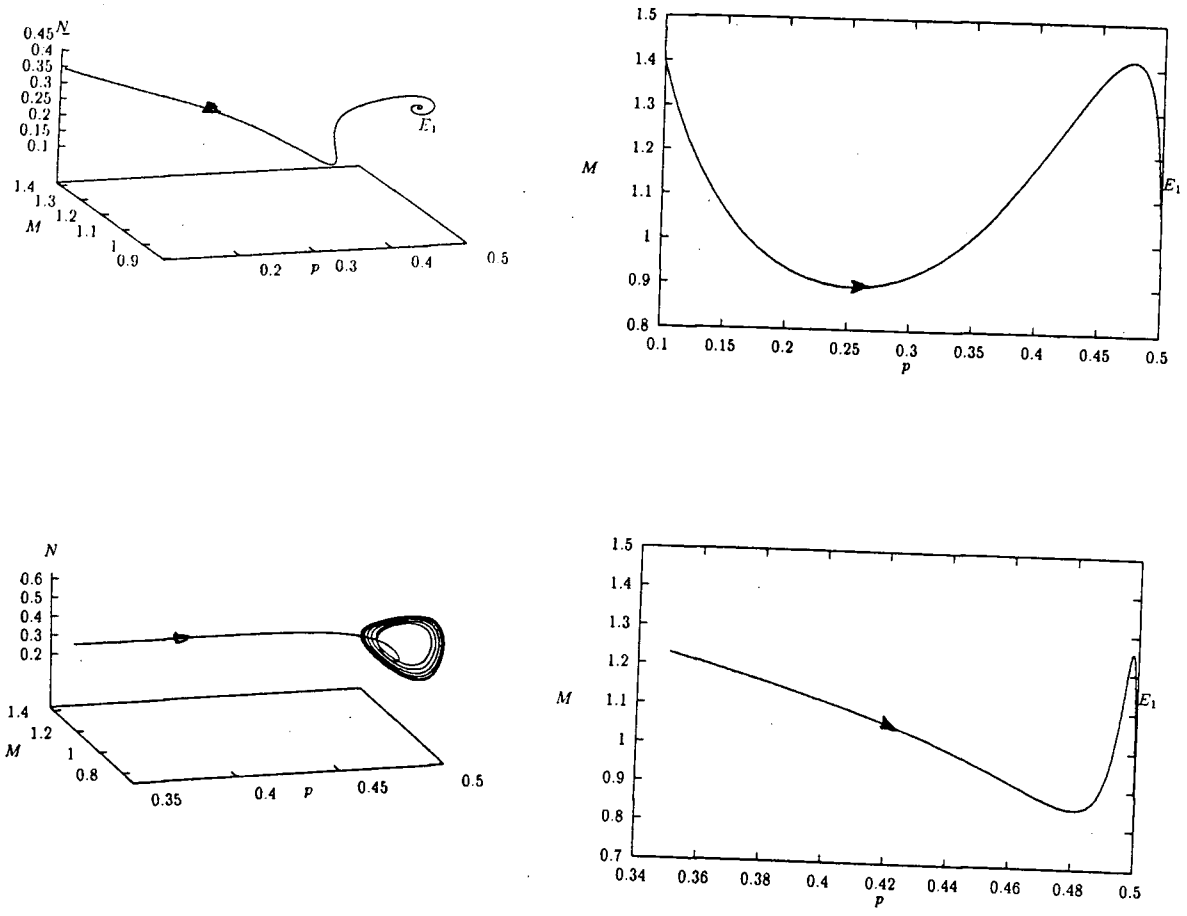

Figure 4.1: Trajectories for continuous-time genetics model with homozygote equality. The parameters used are $a_{AA} = a_{aa} = 0.5$,$a_{Aa} = 1.3$, $b = 0.4$, $c = 2.1$, $c_{22} = 1.1$,$c_{11} = 0.53$ for top diagrams, $c_{11} = 0.4$ for the bottom diagrams. The diagrams on the right are 2-dimensional Mp-plane projections of the graphs on the left. Note that p approaches 0.5 monotonically for both diagrams, and the cycles are on the MN-plane.

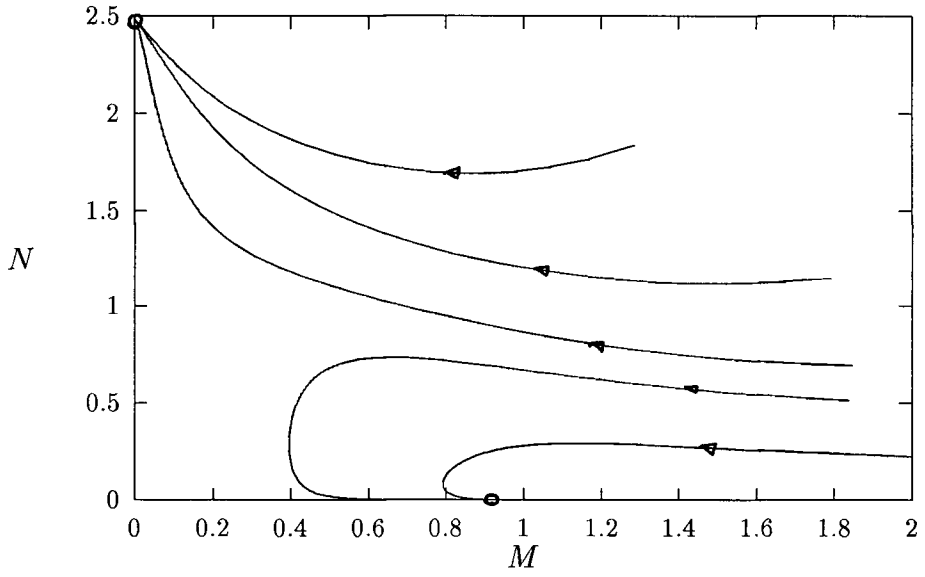

Figure 4.2: Trajectories under loss of genetic variation. Coexistence of the two species is impossible if only one of the homozygotes is present. Extinction of either species depend on initial values. The parameters used are $a_{AA} = a_{aa} = 0.5$, $a_{Aa} = 1.3$, $b = 0.4$, $c = 2.1$, $c_{22} = 1.1$, $c_{11} = 0.53$. And $p(0) = 0$ ($p(0) = 1$ gives same result for homozygote equality)

Next, to show that the Hopf bifurcation is not restricted to homozygote equality, XPPAUT is used to draw bifurcation diagrams by varying a parameter that will remove the homozygote equality. In figure 4.3 the parameter a_{AA}, which initially equaled a_{aa}, is varied together with c_{11} to give a two-parameter bifurcation diagram. When homozygote equality is removed, trajectories are attracted to an invariant manifold that is near $p = 0.5$. For the linear/quadratic model, this equilibrium can be sought explicitly by solving the three equations: $\{\mu_A = \mu_a = \eta = 0\}$.

4.4 Summary

In this chapter, I have been able to show that, with genetic variation added to the pioneer species, not only could there be an stable interior polymorphic equilibrium or a cycle, but that the genetic variation is vital for these to exist. The papers referenced in this

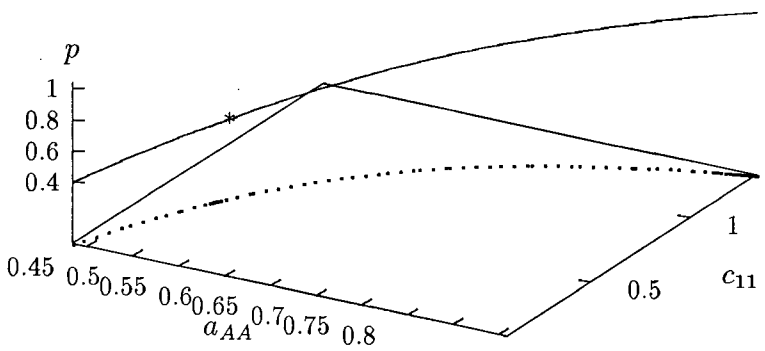

Figure 4.3: Two-parameter continuation, using parameters c_{11} and a_{AA}, of Hopf bifurcations in genetics model (4.1). The parameters used are $a_{Aa} = 1.3$, $a_{aa} = 0.5$, $b = 0.4$, $c = 2.1$. * indicates where the continuation was started: when $a_{AA} = 0.5$ for homozygote equality. The z-axis shows the gene frequency: it is 0.5 at homozygote equality, but changes as the condition is lost.

chapter only considered fitness functions linear in population density, but also those with gene frequency dependence. The model used here as an example is linear for the pioneer, but quadratic for the climax species, and is specific to pioneer-climax competition, which has not been demonstrated in a previously published paper.

Although the dynamics are more complicated with the added dimension, the assumption of homozygote equality effectively reduced the dimension to two again, and allowed reuse of the theory obtained in chapter 2. Since the pioneer fitness for this special case is simply the average of those of the homozygote and the heterozygote, one can quickly find cases where neither the homozygote nor the heterozygote alone can produce a stable coexistence with the competing climax trees, whereas their average can.

Chapter 5

Discrete-time population genetics model

In this chapter, the model of the previous chapter is extended to a 3-dimensional diffeomorphism. The dynamics are expected to be very similar, however, the analysis is more complicated. I am not aware of any papers that deal with this class of model. In Van Coller's [23] thesis, there are two chapters that deal with the same kind of simple genetic variation in a single species: one chapter deals with pioneer type trees, and the other with climax trees. Again, the switch to the discrete-time system is in order to approximate discretely reproducing populations more accurately. I have found again that stable interior polymorphic equilibria or invariant circles can exist, and also that genetic variation is necessary for their existence by means of an example model. When one starts with only one of the two homozygotes, the competitive system excludes one of the two species, depending on the initial coordinates on the phase plane.

In the first section a simple linearization analysis is done to show that, again, local heterozygote superiority is a necessary condition for the occurrence of a Hopf bifurcation. In the second section, the same simplifying assumption, homozygote equality, is considered. Again, this allows us to reduce the dimension of the system using an invariant manifold. Finally in the last section, XPPAUT is used to demonstrate the possibility of a stable interior polymorphic invariant circle, and the consequences of fixation.

5.1 Model equations

As briefly described in the introduction, the dynamics for the gene frequency is slightly changed, and the system of maps becomes

$$(p, M, N) \longmapsto (p\frac{\mu_A}{\mu}, \mu M, \eta N) \tag{5.1}$$

where μ, μ_A, μ_a are defined exactly the same as before, and μ_{ij} are functions of M and N only. Equilibria are found when $\mu = \eta = 1$, so also $\mu_A = \mu_a = 1$. The last two conditions imply that the following must be satisfied:

$$p\mu_{AA} + (1-p)\mu_{Aa} = 1, \tag{5.2}$$

$$p\mu_{Aa} + (1-p)\mu_{aa} = 1. \tag{5.3}$$

Unlike in the ODE case, this does not directly imply that homozygote superiority or inferiority is necessary. The identities of previous chapter, (4.7) and (4.8) still hold, and now the Jacobian at an internal equilibrium $\mathcal{C}$ becomes

$$J(\mathcal{C}) = I + \begin{pmatrix} \frac{\partial}{\partial p}(\mu_A/\mu) & \frac{\partial}{\partial M}(\mu_A/\mu) & \frac{\partial}{\partial N}(\mu_A/\mu) \\ 0 & M\frac{\partial \mu}{\partial M} & M\frac{\partial \mu}{\partial N} \\ 0 & N\frac{\partial \eta}{\partial M} & N\frac{\partial \eta}{\partial N} \end{pmatrix}, \tag{5.4}$$

where I is the three-dimensional identity matrix. The first eigenvalue of the Jacobian is just $1 + \frac{\partial}{\partial p}(\mu_A/\mu)$. Expanding the partial derivatives and employing the identities (4.7) and (4.8) leads to

$$\lambda_1 = 1 + \mu_{AA} - \mu_{Aa}. \tag{5.5}$$

For an interior equilibrium to be stable, all eigenvalues must lie inside the unit circle on the complex plane. Thus for stability we require

$$\begin{aligned} & |1 + \mu_{AA} - \mu_{Aa}| < 1 \\ \Rightarrow \quad & -2 < \mu_{AA} - \mu_{Aa} < 0, \end{aligned} \tag{5.6}$$

which is, again, the heterozygote superiority condition required at the equilibrium since the genotypes AA and aa are symmetric. The other two eigenvalues are from $I_2 + E(C)$ (I_2 is the 2×2 identity matrix), where again, E is the lower right ecology submatrix.

If the total weighted population density variable is the same for each of the pioneer genotypes, that is if $\mu_{ij} = \mu_{ij}(Z)$, then there is a two-dimensional invariant manifold as in chapter 3. If $p \to p_0$, then the function $\mu(Z)$ in chapter 3 becomes

$$\mu(Z) = p_0^2 \mu_{AA}(Z) + 2p_0(1-p_0)\mu_{Aa}(Z) + (1-p_0)^2 \mu_{aa}(Z). \tag{5.7}$$

The same condition $\det C < 0$ must hold for Hopf bifurcation on the invariant manifold. Given that there exists a stable interior equilibrium or invariant circle on the 2-dimensional invariant manifold, they are locally exponentially stable if heterozygote is superior to both homozygotes in that neighborhood.

5.2 Homozygote equality

That $p \to p_0$ exponentially for some $p_0 > 0$ can be demonstrated, as before, if we assume a simplifying condition that the two homozygotes have identical fitness functions. Given that $\mu_{AA} = \mu_{aa}$ then

$$\frac{\mu_A}{\mu} = \frac{p\mu_{AA} + (1-p)\mu_{Aa}}{(2p^2 - 2p + 1)\mu_{AA} + 2p(1-p)\mu_{Aa}}, \tag{5.8}$$

$$\left.\frac{\mu_A}{\mu}\right|_{p=0.5} = 1, \tag{5.9}$$

and one can show that again, $p \to 0.5$ as $t \to \infty$. A simple coordinate transformation $p = \frac{1}{2} + r$ takes the map for p to

$$r \longmapsto \frac{\mu_A}{\mu}(r + \frac{1}{2}) - \frac{1}{2} \tag{5.10}$$

$$\longmapsto \frac{r(\mu_{AA} - \mu_{Aa}) + \frac{1}{2}(\mu_{AA} + \mu_{Aa})}{2r^2(\mu_{AA} - \mu_{Aa}) + \frac{1}{2}(\mu_{AA} + \mu_{Aa})} \tag{5.11}$$

$$\longmapsto \frac{2\mu_{AA}}{\mu_{AA} + \mu_{Aa}} r + \mathcal{O}(r^2) \tag{5.12}$$

so that if $\mu_{Aa} - \varepsilon > \mu_{AA}$ for some $\varepsilon > 0$, then the coefficient in front of r is strictly between 0 and 1, so the two-dimensional manifold $r = 0$, or equivalently $p = 0.5$, is exponentially stable. So again, the three dimensional system reduces to $p = 0.5$ and

$$(M, N) \longmapsto ((\mu_{AA} + \mu_{Aa})M/2, \eta N). \tag{5.13}$$

As before, if both μ_{AA} and μ_{Aa} are functions of the same weighted total density Z, then (5.13) is exactly the same system described and analyzed in chapter 4. Thus there would a be stable interior polymorphic equilibrium or an invariant circle given the same conditions given in that chapter. If the Z_{ij} are different, then for homozygote equality the analysis would be similar to the one given in chapter 4, but more complex. However, this case is not considered in this thesis. In the next section an exponential fitness function is analyzed using XPPAUT.

5.3 Numerical example

Consider the following exponential model:

$$\mu_{ij}(Z) = e^{(a_{ij}-Z)}, \tag{5.14}$$

$$\eta(W) = We^{(b-W)}. \tag{5.15}$$

Figure 5.1 shows the trajectories before and after Hopf bifurcation at E_1 for homozygote equality. Again, to show that the Hopf bifurcation is not restricted to homozygote equality, a two-parameter bifurcation is computed using XPPAUT. Figure 5.2 shows the two-parameter (c_{11} and a_{AA}) bifurcation diagram for the Hopf bifurcation at E_1, plotted against the equilibrium p in the z-axis. Note that heterozygote superiority is lost as a_{AA} increases past a_{Aa}.

While it is not analytically obvious, it can again be demonstrated that in this model, genetic variation may be crucial in making a stable interior equilibrium possible. If there

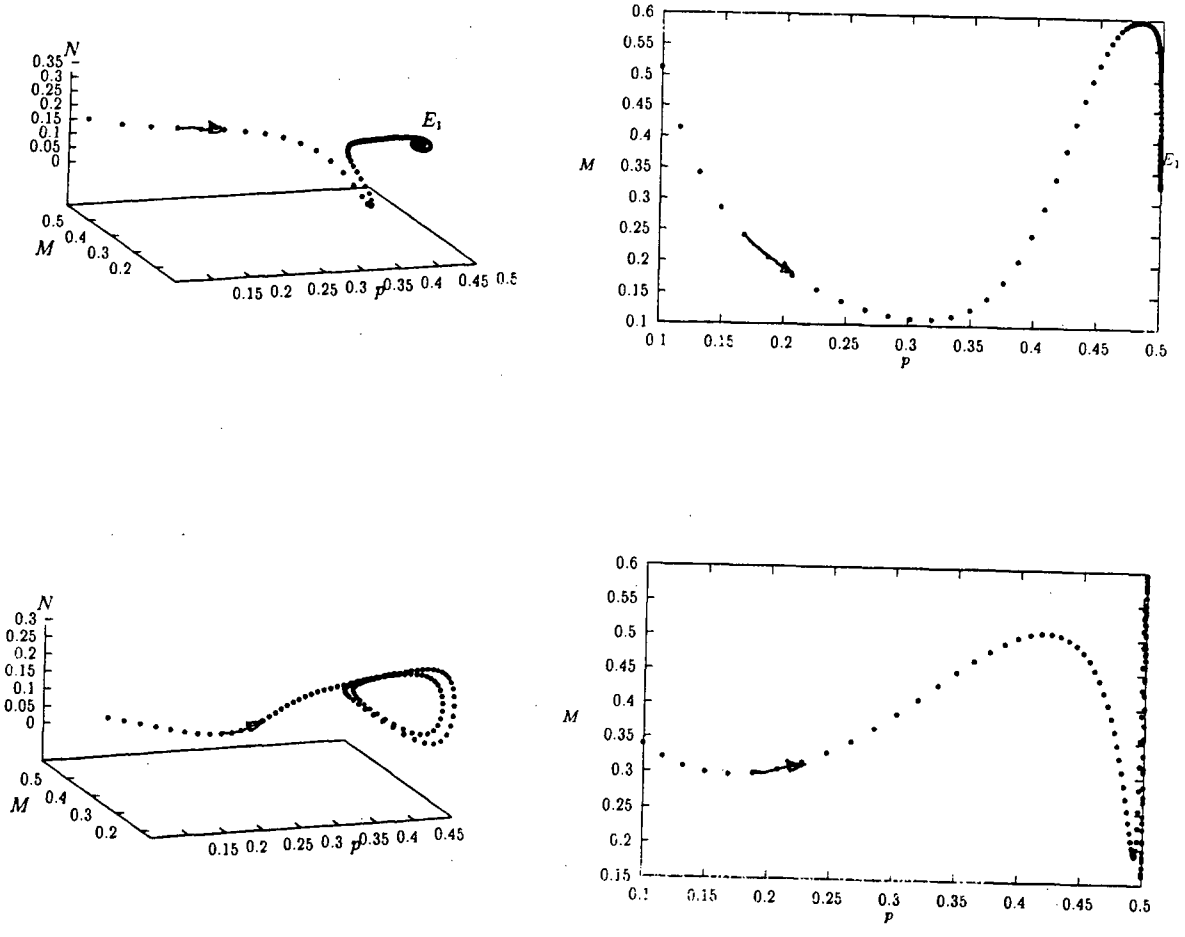

Figure 5.1: Trajectories for discrete-time genetics model, before and after Hopf bifurcation. The parameters are $c_{22} = 1$, $a_{AA} = a_{Aa} = 0.2$, $a_{Aa} = 0.4$, $b = 1.2$, with $p(0) = 0.1$. The parameter $c_{11} = 0.5$ for the top diagrams, and c_{11}=4.3 for the bottom diagrams. The diagrams on the right show the same trajectories projected onto the Mp-plane. Note that p approaches 0.5 monotnonically.

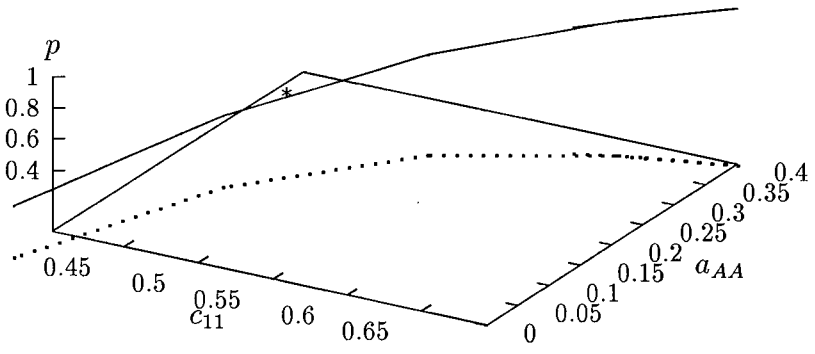

Figure 5.2: Two parameter continuation of Hopf bifurcation for the discrete-time model. The other constant parameter values are the same as in figure 5.1. The mark * indicates where the continuation was initiated, at homozygote equality ($a_{AA} = a_{aa} = 0.2$). The vertical axis shows the equilibrium p value.

is only one of the homozygotes present initially, the system would exclude either species depending on the initial values, making stable coexistence impossible. Using the same model as above, consider trajectories starting with $p = 0$ or $p = 1$. As it can be seen from figure 5.3 below, in either case there is no longer a stable interior equilibrium, but the species exclude each other depending on the initial condition.

5.4 Summary

The results of this chapter are very similar to those of chapter 4. I have shown, through an analogous analysis to that of chapter 4, that there exists a stable interior polymorphic equilibrium or invariant circle, given the simplifying homozygote equality condition. I have also shown numerically that homozygote equality is not necessary for stable coexistence. Moreover, a numerical example showed a case where the genetic variation is

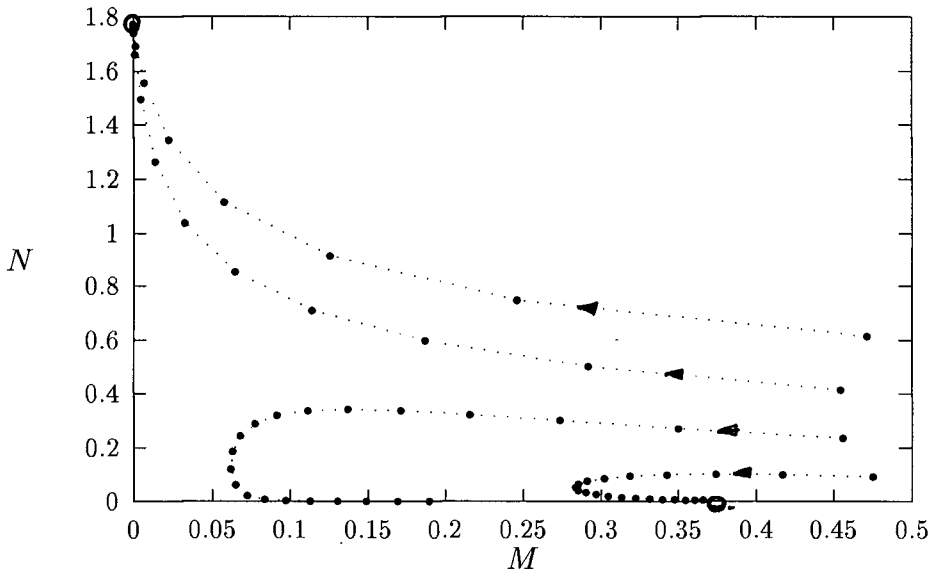

Figure 5.3: Trajectories under loss of genetic variation. The trajectories here for competition between climax and either of the homozygotes shows that the species exclude each other, depending on the initial condition. The parameter values are the same as those used in the top diagram of figure 5.1

a necessity in obtaining such an equilibrium: coexistence becomes impossible when the system initially starts with either of the homozygotes only.

Chapter 6

Genetic variation on both species

Finally, I consider a four-dimensional system of ODEs, which includes genetic variation in both the pioneer and the climax species. In addition to the density variable M and N, there are the two gene-frequency variables p and q for the A allele in the pioneer species and B allele for the climax species, respectively. This model can be considered a generalization of the one in chapter 4, since fixation in the climax species will reduce to the same model.

Selgrade and Namkoong [17] deal with this type of competition, and derive general results. The paper show some examples where stable periodic solutions are possible for species exhibiting a predator-prey interaction, when the fitnesses are functions of population densities only. In this chapter, I survey the analytical results of the paper, then give a new example specific to pioneer-climax competition. I show that there can be a stable polymorphic interior equilibrium or cycle in the four dimensions. As well, I give some example where there cannot be a stable coexistence in the absence of genetic variation in one or both species.

6.1 Model equations

The alleles for the climax population are B and b, and the gene-frequencies are q and $1-q$ respectively. There are six distinct fitness functions of weighted total population density, $\mu_{AA}(Z^{AA})$, $\mu_{Aa}(Z^{Aa})$, $\mu_{aa}(Z^{aa})$, $\eta_{BB}(W^{BB})$, $\eta_{Bb}(W^{Bb})$, $\eta_{bb}(W^{bb})$.

The system of ODEs now looks like:

$$\begin{aligned}
\dot{p} &= p(\mu_A - \mu) = p(1-p)(\mu_A - \mu_a), \\
\dot{q} &= p(\eta_B - \eta) = p(1-p)(\eta_B - \eta_b), \\
\dot{M} &= \mu M, \\
\dot{N} &= \eta N,
\end{aligned} \tag{6.1}$$

where the marginal fitnesses μ_A, μ_a, η_B, η_b and average fitnesses μ and η are defined exactly same as before:

$$\eta_B = q\eta_{BB} + (1-q)\eta_{Bb}, \tag{6.2}$$

$$\eta_b = q\eta_{Bb} + (1-q)\eta_{bb}, \tag{6.3}$$

$$\eta = q\eta_B + (1-q)\eta_b. \tag{6.4}$$

The definitions for the pioneer population are already given in chapter 4. The derivative identities also hold:

$$\frac{\partial \eta}{\partial q} = 2(\eta_B - \eta_b), \tag{6.5}$$

$$\frac{\partial^2 \eta}{\partial q^2} = 2(\eta_{BB} - 2\eta_{Bb} + \eta_{bb}). \tag{6.6}$$

At an equilibrium, we must have $\mu_A = \mu_a = \eta_B = \eta_b = 0$. This implies again that either heterozygote superiority or inferiority must hold for both species. The Jacobian at an equilibrium E is:

$$J(E) = \begin{pmatrix}
\frac{1}{2}p(1-p)\frac{\partial^2 \mu}{\partial p^2} & 0 & p(1-p)\frac{\partial(\mu_A - \mu_a)}{\partial M} & p(1-p)\frac{\partial(\mu_A - \mu_a)}{\partial N} \\
0 & \frac{1}{2}q(1-q)\frac{\partial^2 \eta}{\partial q^2} & q(1-q)\frac{\partial(\eta_B - \eta_b)}{\partial M} & q(1-q)\frac{\partial(\eta_B - \eta_b)}{\partial M} \\
0 & 0 & M\frac{\partial \mu}{\partial M} & M\frac{\partial \mu}{\partial N} \\
0 & 0 & N\frac{\partial \eta}{\partial M} & N\frac{\partial \eta}{\partial N}
\end{pmatrix} \tag{6.7}$$

The first two eigenvalues are identified immediately:

$$\lambda_1 = p(1-p)(\mu_{AA} - 2\mu_{Aa} + \mu_{aa}), \tag{6.8}$$

$$\lambda_2 = q(1-q)(\eta_{BB} - 2\eta_{Bb} + \eta_{bb}), \tag{6.9}$$

and the remaining two are again, the eigenvalues of the lower right 2×2 ecology matrix. For an equilibrium to be stable, the eigenvalues must all have negative real parts, so this clearly means there must be heterozygote superiority for both populations at the equilibrium, employing the same analysis as in chapter 4.

6.2 Hopf Bifurcation

Consider the ecology matrix:

$$E(C) = \begin{pmatrix} M\frac{\partial \mu}{\partial M} & M\frac{\partial \mu}{\partial N} \\ N\frac{\partial \eta}{\partial M} & N\frac{\partial \eta}{\partial N} \end{pmatrix} \tag{6.10}$$

The trace and determinant of the matrix are exactly the same as given in chapter 4, equations (4.12) and (4.13). The difference is that now η is no longer a simple function of population densities, but also involves genetic frequency of the B allele. One cannot say for certain this time, that $\frac{\partial \eta}{\partial M}$ or $\frac{\partial \eta}{\partial N}$ at an equilibrium is positive, since a nonnegative sum of unimodal functions are not necessarily unimodal. However, the fitness functions of the three genotypes of the climax species cannot have so large a difference, and one might assume safely that $\frac{\partial \eta}{\partial N}, \frac{\partial \eta}{\partial M} > 0$ for competition at the smaller of the two equilibria.

6.3 Homozygote equality

Again, the analysis is much simplified when we assume homozygote equality for both species ($\mu_{AA} = \mu_{aa}$, $\eta_{BB} = \eta_{bb}$). Skipping a detailed analysis, the assumption makes $p =$

$q = 0.5$ exponentially stable (a simple coordinate transformation $p = \hat{p} + 1/2, q = \hat{q} + 1/2$ will show this), thus reducing the system of equations to second order in M and N:

$$\begin{aligned} \dot{M} &= \frac{1}{2}(\mu_{AA} + \mu_{Aa})M \\ \dot{N} &= \frac{1}{2}(\eta_{BB} + \eta_{Bb})N. \end{aligned} \tag{6.11}$$

If we assume further that the weighted density variables for each genotype in the respective species are identical (i.e., $Z^{AA} = Z^{Aa}$ and $W^{BB} = W^{Bb}$) then the results of chapter 2 may hold directly. There is a possibility, in case the homozygote and heterozygote fitness differ greatly, that their average will not be a simple unimodal function. However, this is probably not biologically realistic. So again, one would expect there to be at most two interior equilibria, and Hopf bifurcation would occur at the smaller equilibrium by varying either c_{11} or c_{22}.

6.4 Numerical example using XPPAUT

Exponential models are again considered here:

$$\mu_{ij}(Z^{ij}) = e^{(a_{ij} - Z^{ij})} - 1, \tag{6.12}$$

$$\eta_{ij}(W^{ij}) = W^{ij} e^{(b_{ij} - W^{ij})} - 1. \tag{6.13}$$

For simplicity, assume identical density variables ($Z^{AA} = Z^{Aa}$ and $W^{BB} = W^{Bb}$). With homozygote equality, one can easily find the equilibrium E_1 using nearly the same parameters as the example in chapter 2, only choosing a_{AA} and a_{Aa} so that their average equals a in chapter 2, and similarly choosing b_{BB} and b_{Bb} such that their average will equal b in the model in chapter 2. For the diagram in figure 6.1, I chose $p(0) = 0.1$ and $q(0) = 0.9$ to demonstrate how the gene frequencies approach 0.5 while on the MN-plane, the trajectories either approach an interior equilibrium, or approach a stable periodic orbit. Hopf

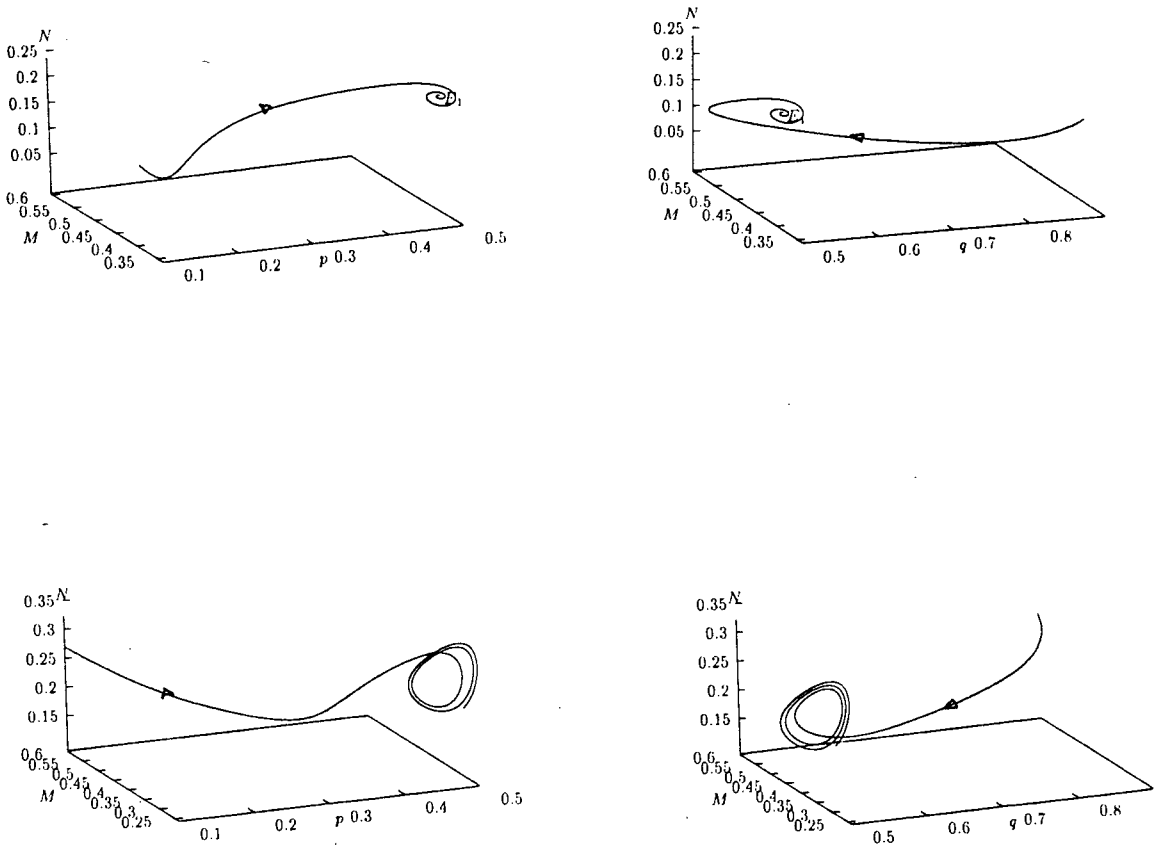

Figure 6.1: Trajectories for the four-dimensional continuous-time model with genetic variation in both species, before and after Hopf bifurcation. The top two diagrams show a stable interior polymorphic equilibrium: on the left p approaces 0.5 from the inital 0.1; on the right q approaches 0.5 from the initial 0.9. The two bottom diagrams show similar results after a Hopf bifurcation in the MN-plane. The parameters are $a_{AA} = a_{aa} = 0.3, a_{Aa} = 0.5, b_{BB} = b_{bb} = 0.9, b_{Bb} = 1.3$, $c_{22} = 1$; $c_{11} = 0.53$ for top diagrams, $c_{11} = 0.44$ for the bottom diagrams.

bifurcation is persistent under small perturbations, so it will still occur after homozygote equality is removed for either or both species. This fact is shown in figure 6.2, which is a two-parameter bifurcation diagram in a_{AA} and b_{BB}. Curve i on the diagram is the interior polymorphic Hopf bifurcation: note that it ceases to exist as heterozygote superiority is lost (a_{AA} goes beyond $a_{Aa} = 0.5$), and it is taken over by another Hopf bifurcation curve iii, which is the one for the case $p = 1$. Curve ii goes into unrealistic regions when it approaches tangentially curve iv, which is another Hopf bifurcation curve for the fixation $p = 1$ and $q = 1$. Finally, curve ii is a Hopf bifurcation curve for the case $q = 1$. Note that inside the lower left rectangle bounded by the dotted lines, heterozygote superiority holds for both species, so $p = 1$ and $q = 1$ are unstable, though invariant.

Finally, the effect of fixation, that is, loss of genetic variation in either or both species, is demonstrated. The trajectories in figure 6.3 shows the case when the initial gene frequencies are $p(0) = 0$ and/or $q(0) = 0$. The interior equilibrium is no longer possible in this case, and the species exclude each other depending on the initial values. It is seen that for the particular parameter values, there is a global exclusion of the climax species when $q(0) = 1$ and $p(0) = 0.5$.

6.5 Summary

In this chapter I was able to show that there exists stable interior polymorphic equilibrium or cycle when the pioneer and the climax species compete with genetic variation on both species. Moreover, I found that these could vanish when the variation is removed for either species at homozygote equality.

The result of the two-parameter bifurcation diagram in figure 6.2 reveals that interior polymorphic equilibria and cycles are not restricted to homozygote equality, but persists when the condition is removed, by varying a_{AA} and b_{BB}. The two-parameter continuation

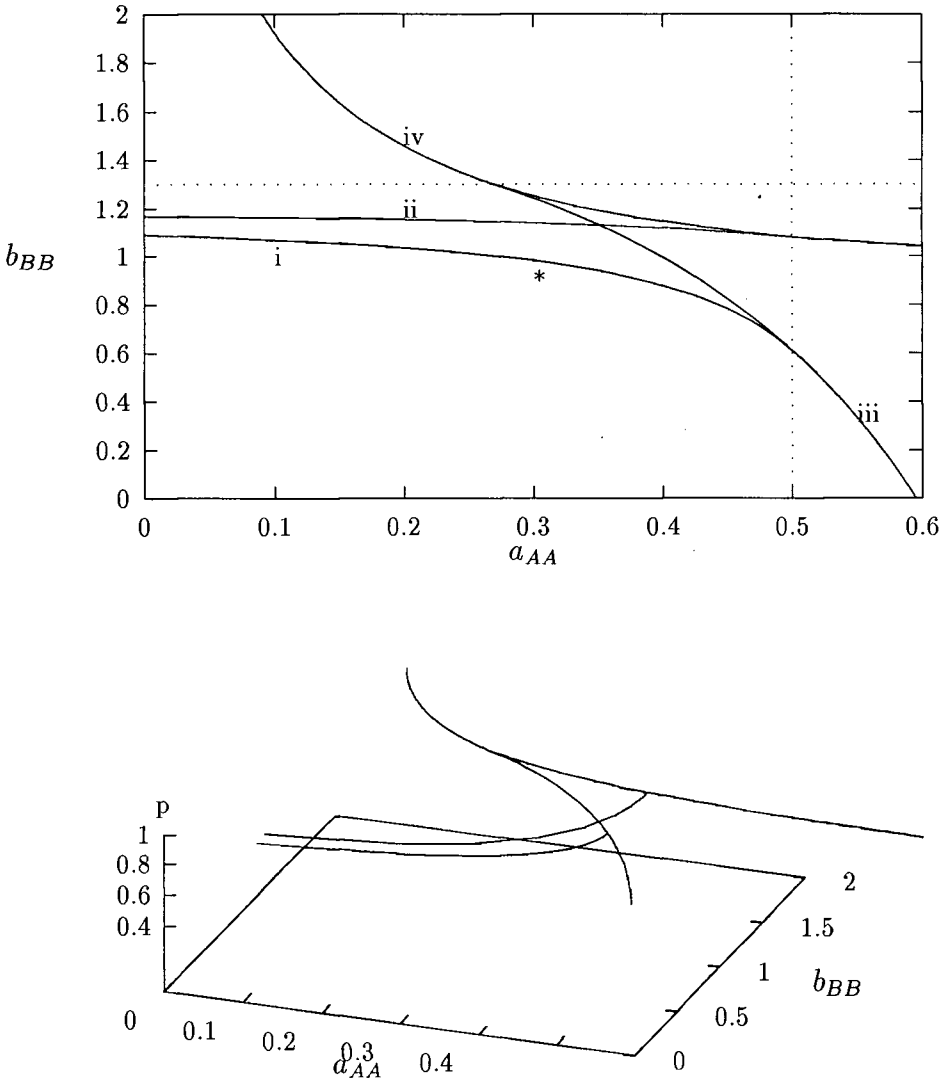

Figure 6.2: Hopf bifurcation diagram in two parameters: a_{AA} and b_{BB}. The other parameters are $a_{12} = 0.5$, $a_{22} = 0.3$, $b_{12} = 1.3$, $b_{22} = 0.9$, $c_{11} = 0.53$, $c_{22} = 1$. Curve i is for polymorphic Hopf bifurcation; ii is Hopf bifurcation for when $q = 1$; iii is Hopf bifurcation corresponding to $p = 0$; curve iv is Hopf bifurcation on the fixation plane $p = 1, q = 1$. The bottom diagram shows the same curves in three dimensions with p plotted along the vertical axis. The label * indicates where homozygote equality holds for both species.

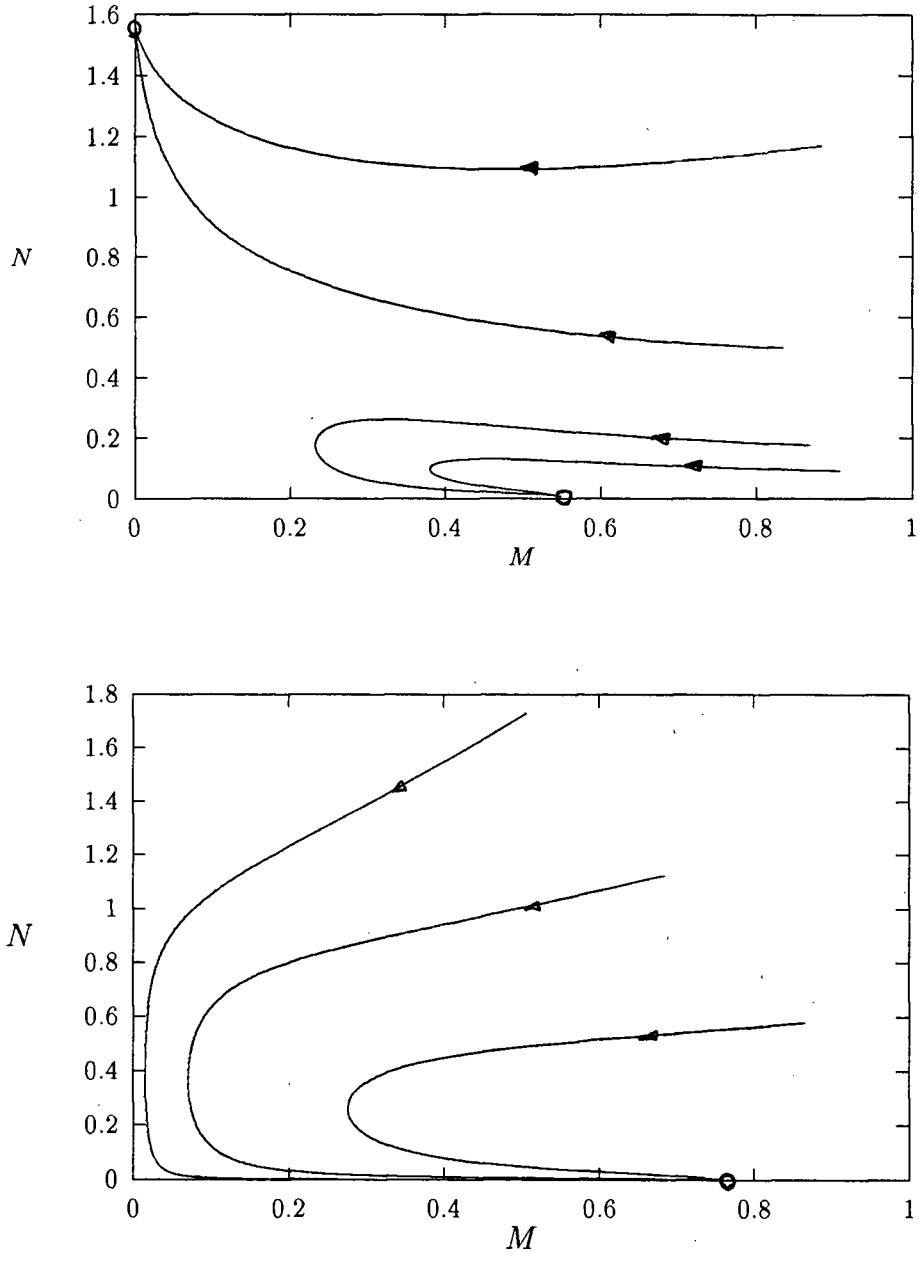

Figure 6.3: Trajectories under loss of genetic variation. The parameters used are the same as the top diagrams in figure 6.1. The difference is that the initial value of $p(0) = 0, q(0) = 0.5$ is used for the top diagram and $p(0) = 0.5, q(0) = 0$ is used for the bottom diagram.

discovered other Hopf bifurcation curves which correspond to $p = 1$ or $q = 1$. Thus for some parameter values, specifically when a homozygote is superior to the heterozygote, stable coexistence is possible even under loss of genetic variation.

Chapter 7

Conclusion

This thesis has two main components. In the first half (chapters 2 and 3) I have surveyed the results of theoretical analysis by different papers on a non-genetical pioneer-climax competition, then proceeded to give numerical examples using the software package XP-PAUT. In the second half (chapters 4, 5 and 6) I have applied some ideas on general competition models with genetic variation in one of the two competing species to competition of the pioneer-climax type. Some numerical examples were also given.

The primary interest of the first half was to examine the qualitative behavior of competition between two species of trees with different parameters. It has been observed in reality that often the climax species exclude the pioneer species, but also that occasionally the species apparently coexist. Thus, information regarding what conditions allow for coexistence or periodic interior behavior is important.

The second half is devoted to competition with genetic variation. The main question here is what are the situations (parameter combinations) that allow interior, polymorphic equilibria or cycles, which would be impossible at either fixation plane ($p = 0$ or $p = 1$). While there have been papers that examined this question using some models in continuous time, there has not been the equivalent in discrete time, nor any that are specific to pioneer-climax competition. This thesis makes some analogous analysis for the discrete-time case, as well as presenting numerical examples for both continuous- and discrete-time cases.

There is a lack of correspondence with real data. Although the systems examined

in the thesis are very simplified, and only qualitative results at best can be expected, it would have been nice to have 'reasonable' parameters at hand to see the likelihood of different events occurring in the parameter space. The reasonable parameters are unknown to me, because of lack of research into real data that may be already available as published literature.

7.1 Further research

I have only looked at density dependent fitness functions in the genetic models, although fitnesses involving the gene frequency are also possible. Another question to be addressed is the 'control' aspect of these models. Given a model that describes a system of competition under 'natural' conditions, one can add control terms which might correspond to harvesting or planting. While 'optimal' control may be difficult to analyze by hand, simple harvesting or planting terms can be added in order to examine their effects. For non-genetic competition, Yakubu [24] and Selgrade [14] show how different stocking or harvesting can reverse possible undesirable behavior, or bring coexistence of species into a system that otherwise excludes one of the species. Similar control terms can be added to the genetic models, possibly some that alter population density as well as gene frequency by selectively planting or harvesting different genotypes.

A natural extension of chapter 6 is to take the system to four dimensional diffeomorphism, which should produce similar results.

Finally, an interesting study would be a spatial model. For the non-spatial model we assume homogeneous distributions for trees of both species, which is often a good approximation. However, it would be fruitful to study any effect of spatial imbalance, or effect of control terms which would plant or remove trees of either species in different spatial areas.

Bibliography

[1] J. F. Crow and M. Kimura. *An Introduction to Population Genetics Theory.* Harper and Row, New York, 1970.

[2] B Ermentrout. The differential equations tool (user manual). *Unpublished. Available at ftp.math.pitt.edu/pub/bardware.*

[3] J. E. Franke and A. Yakubu. Mutual exclusion versus coexistence for discrete competitive systems. *J. Math. Biol.*, 30:161, 1991.

[4] J. E. Franke and A. Yakubu. Pioneer exclusion in a one-hump discrete pioneer-climax competitive system. *J. Math. Biol.*, 32:771, 1994.

[5] L. R. Ginzburg. *Theory of Natural Selection and Population Growth.* Menlo Park Benjamin/Cummings, 1983.

[6] B. D. Hassard, N. D. Kazarinoff, and H. Wan, Y. *Theory and Applications of Hopf Bifurcation.* Cambridge Univ. Press, New York, 1981.

[7] Y. A. Kuznetsov. *Elements of applied bifurcation theory.* Springer-Verlag, New York, 1995.

[8] S. A. Levin and J. D. Udovic. A mathematical model of coevolving populations. *Amer. Nat*, 11:657, 1977.

[9] R. M. May. Simple mathematical models with very complicated dynamics. *Nature*, 261:459, 1976.

[10] R. M. May and G. Oster. Bifurcations and dynamic complexity in simple ecological models. *Amer. Nat.*, 110:573, 1976.

[11] J. D. Murray. *Mathematical Biology.* Springer-Verlag, New York, 1989.

[12] J. Roughgarden. *Theory of Population Genetics and Evolutionary Ecology: An Introduction.* MacMillan, New York, 1979.

[13] J. F. Selgrade. Period-doubling bifurcations for systems of difference equations and applications to models in population biology. *Preprint*, 1996.

[14] J. F. Selgrade. Using stocking or harvesting to reverse period-doubling bifurcations in models of population interactions. *Preprint*, 1996.

[15] J. F. Selgrade and G. Namkoong. Dynamical behavior of differential equation models of frequency and density dependent populations. *J. Math. Biol.*, 19:133, 1984.

[16] J. F. Selgrade and G. Namkoong. Examples of the effect of genetic variation on competing species. *J. Math. Biol.*, 24:193, 1986.

[17] J. F. Selgrade and G. Namkoong. Stable periodic solutions for two species, density dependent coevolution. *J. Math. Biol.*, 22:69, 1986.

[18] J. F. Selgrade and G. Namkoong. Stable periodic behavior in a pioneer-climax model. *Nat. Res. Modeling*, 4:215, 1990.

[19] J. F. Selgrade and G. Namkoong. Planting and harvesting for pioneer-climax models. *Rocky Mountain J. Math.*, 24:193, 1993.

[20] J. F. Selgrade and J. H. Roberds. Lumped-density population models of pioneer-climax type and stability analysis of hopf bifurcations. *Preprint*, 1996.

[21] S. Sumner. Competing species models for pioneer-climax forest dynamical systems. *Proc. Dynam. Systems Appl.*, 1:351, 1994.

[22] S. Sumner. Hopf bifurcation in pioneer-climax competing species models. *Math. Biosc.*, 137:1, 1996.

[23] L. Van Coller. *Qualitative Analyses of Ecological Models - An Automated Dynamical Systems Approach.* PhD thesis, The University of British Columbia, 1996.

[24] A-A. Yakubu. The effects of planting and harvesting on endangered species in discrete competitive systems. *Math. Biosc.*, 126:1, 1994.

Appendix A

The software package XPPAUT

There are several software packages available today for analyzing system of equations, such as AUTO, AUTO90, Interactive AUTO and XPPAUT [2]. The last two are basically graphical interfaces to AUTO to facilitate computation. Of these, XPPAUT is especially easy to use, because it combines both the functionality of phase-plane plotting with the ability of AUTO to produce bifurcation diagrams. In order to produce such bifurcation diagrams as those presented in this thesis, the programs 'continue' a given equilibrium by varying a given parameter. The procedure that was used, is to (1) find an equilibrium point (stable or unstable) using the phase-plotting functionality of XPPAUT, then (2) transfer the equilibrium to the AUTO interface, and continue the point by varying a parameter. For the two-parameter bifurcation diagram of Hopf bifurcations, a bifurcation point is first located using a one-parameter procedure, then the bifurcation is continued along the two parameter plane.

The advantages of doing a bifurcation analysis are obvious. Instead of doing numerous simulations by choosing many possible parameter combinations, one can find ranges of qualitative behaviors in up to two parameters. Even in a system with many parameters, one can explore different qualitative behavior by taking many two-dimensional cross sections in the parameter space. While the parameters are regarded as constant in the equations, it is often the case that they are dynamic in reality, which makes single-shot simulations less useful. By examining a bifurcation diagram, and by considering how a parameter would change slowly in time, useful predictions can be made on the changes in

qualitative behavior. For example, if carrying capacity is expected to increase slowly in time, then a bifurcation diagram in the parameter representing carrying capacity would show how behavior might change.

XPPAUT is available from an anonymous ftp: ftp.math.pitt.edu/pub/bardware. There is also an online tutorial is also available at the same site. One copy of the tutorial is located at http://www.iam.ubc.ca/guides/xppaut/start.html.

A.1 Numerical details

AUTO uses what is known as a predictor-corrector method to continue an equilibrium or periodic orbit. The method involves two steps: first an approximation to the next point on the curve is made, using a vector tangent to the previous point. This is the predictor step. Next, the approximation is improved (i.e, corrected) by iteration, using Newton's method. The bifurcation curve needs to be parameterized, and this is done using a pseudo-arclength.

Meanwhile, the eigenvalues of the Jacobian matrix and a test function to detect bifurcations are monitored (Floquet multipliers are monitored for periodic orbits). For ODEs, while all the real parts of the eigenvalues are negative, the equilibrium is stable, and AUTO indicates this by drawing thick lines (filled dots for periodic orbits), and when one or more of the eigenvalues have positive real part, the equilibrium is unstable, and the lines are dotted. For maps, the eigenvalues are monitored if they are inside or outside the unit circle.

To detect a bifurcation point, AUTO uses an indirect method using a test function, say f. When the sign of the test function changes, there is a bifurcation. An example is $f = \alpha_k, |\alpha_k| = min\{|\alpha_1|, ..., |\alpha_m|\}$, where α_i are the eigenvalues.

The accuracy of the computations depend on the stepsize used for the predictor step.

AUTO uses an adaptive strategy for varying the stepsize: while the corrective iterations are converging rapidly, a large predictor stepsize is taken, and when the iterations converge slowly, the predictive stepsize is decreased. The user can choose the minimum and maximum stepsize to be taken.

On the practical side, in order to produce the diagrams in this thesis, the AUTO output file, typically named *.p, is manipulated and its result is plotted using a plotting software like gnuplot.

A.2 XPPAUT Listings

Below are the XPPAUT input files that were used to produce the diagrams in the thesis. Note that there is an 'old' way and a 'new' way to write these files, and the ones below are mixtures of the two. The ODE files have extensions **.ode*, while diffeomorphisms have extensions **.dif*. Please refer to the manual for details.

- XPPAUT file for the example in chapter 2 (ch2.ode)

```
dm/dt=mu(m,n)*m
dn/dt=eta(m,n)*n
par a=.5,b=.4,c11=0.3,c22=1.1
z(m,n)=c11*m+n
w(m,n)=m+c22*n


mu(m,n)=exp(a-z(m,n))-1
eta(m,n)=w(m,n)*exp(b-w(m,n))-1
done
```

- XPPAUT file for the example in chapter 3 (ch3.dif)

```
2


v x,y
p a=1, b=1, c11=1,c22=1
o x*exp(a-(c11*x+y))
o y*(x+c22*y)*exp(b-(x+c22*y))


done
```

- XPPAUT file for the example in chapter 4. (ch4.ode)

```
dp/dt=p*(1-p)*(w1(p,m,n)-w2(p,m,n))
dm/dt=u(p,m,n)*m
dn/dt=(b-(w(m,n)-g)^2)*n
par a11=.5,a12=1.3,a22=.5, b=.4,g=2.1,c11=0.53,c22=1.1
z(m,n)=c11*m+n
w(m,n)=m+c22*n
w11(m,n)=a11-z(m,n)
w12(m,n)=a12-z(m,n)
w22(m,n))=a22-z(m,n)
w1(p,m,n)=p*w11(m,n)+(1-p)*w12(m,n)
w2(p,m,n)=p*w12(m,n)+(1-p)*w22(m,n)
u(p,m,n)=p*w1(p,m,n)+(1-p)*w2(p,m,n)
done
```

4. XPPAUT file for the example in chapter 5. (ch5.dif)

```
p(t+1)= p*w1(p,m,n)/fitmean(p,m,n)
```

```
m(t+1)= m*fitmean(p,m,n)
n(t+1)= n*(m+c22*n)*exp(b-m-c22*n)

w11(m,n) = exp(a11-b11*(c11*m-n))
w12(m,n) = exp(a12-b12*(c11*m-n))
w22(m,n) = exp(a22-b22*(c11*m-n))
w1(p,m,n) = p*w11(m,n)+(1-p)*w12(m,n)
w2(p,m,n) = p*w12(m,n)+(1-p)*w22(m,n)
fitmean(p,m,n) = p*w1(p,m,n)+(1-p)*w2(p,m,n)

param c11=0.5,c22=1,a11=2.1,a12=1.9,a22=1.1,b=1.2,b11=1,b12=1,b22=1

p(0)=0.5
m(0)=0.3765
n(0)=0.11674

done
```

5. XPPAUT file for the example in chapter 6. (ch6.ode)

```
dp/dt=p*(1-p)*(w1(p,m,n)-w2(p,m,n))
dq/dt=q*(1-q)*(y1(q,m,n)-y2(q,m,n))
dm/dt=u(p,m,n)*m
dn/dt=eta(q,m,n)*n
par a11=.3,a12=0.5,a22=.3, b11=.9,b12=1.3,b22=0.9,c11=0.53,c22=1
z(m,n)=c11*m+n
w(m,n)=m+c22*n
```

```
w11(m,n)=exp(a11-z(m,n))-1
w12(m,n)=exp(a12-z(m,n))-1
w22(m,n))=exp(a22-z(m,n))-1
w1(p,m,n)=p*w11(m,n)+(1-p)*w12(m,n)
w2(p,m,n)=p*w12(m,n)+(1-p)*w22(m,n)
u(p,m,n)=p*w1(p,m,n)+(1-p)*w2(p,m,n)

y11(m,n)=w(m,n)*exp(b11-w(m,n))-1
y12(m,n)=w(m,n)*exp(b12-w(m,n))-1
y22(m,n)=w(m,n)*exp(b22-w(m,n))-1
y1(q,m,n)=q*y11(m,n)+(1-q)*y12(m,n)
y2(q,m,n)=q*y12(m,n)+(1-q)*y22(m,n)
eta(q,m,n)=q*y1(q,m,n)+(1-q)*y2(q,m,n)
done
```